

REPORT No. 907

EQUATIONS FOR THE DESIGN OF TWO-DIMENSIONAL SUPERSONIC NOZZLES

By I. IRVING PINKEL

SUMMARY

Equations are presented for obtaining the wall coordinates of two-dimensional supersonic nozzles. The equations are based on the application of the method of characteristics to irrotational flow of perfect gases in channels. Curves and tables are included for obtaining the parameters required by the equations for the wall coordinates.

A brief discussion of characteristics as applied to nozzle design is given to assist in understanding and using the nozzle-design method of this report. A sample design is shown.

INTRODUCTION

A supersonic nozzle is used to transform parallel flow at sonic velocity into parallel, uniform flow at a supersonic Mach number. The conventional two-dimensional supersonic nozzle consists of the following four main parts arranged in the direction of flow (fig. 1):

- (1) A subsonic inlet converging in the direction of flow
- (2) A throat in which the streamlines are parallel to the nozzle axis and sonic velocity of the compressible flow is reached
- (3) An expanding part with constant or increasing angle of inclination of the nozzle wall to the axis of the nozzle, in which the flow accelerates to supersonic speeds
- (4) A straightening part of increasing area of cross section in the direction of flow but decreasing angle of in-

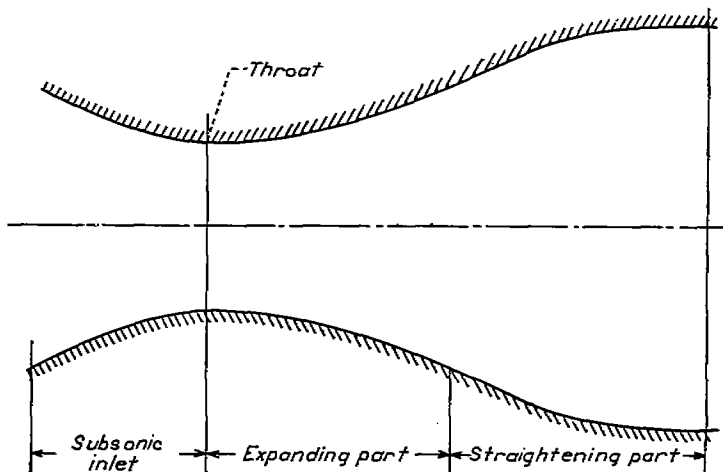


FIGURE 1.—Parts of conventional supersonic nozzle.

clination of the wall to the nozzle axis; in this part, the flow is turned parallel to the nozzle axis with the desired final Mach number uniform across the exit section.

In a properly designed nozzle, there are no compression or expansion waves in the flow downstream of the straightening portion. A streamline crossing such waves would be altered in direction and Mach number, which is generally undesirable.

The method of characteristics provides a means for obtaining the properties of a fluid moving at supersonic speed past solid surfaces. A particular application of the method of characteristics permits the solution of the inverse problem of obtaining the profile of the solid boundary that would create a desired supersonic flow.

Graphical methods for designing two-dimensional nozzles by the method of characteristics, for example, are reviewed in reference 1. Graphical methods employing characteristics for obtaining nozzles free from waves in the final flow, however, are tedious and subject to the error inherent in construction involving the plotting of many consecutive lines.

The application of the method of characteristics to the analytical design of two-dimensional supersonic nozzles was completed at the NACA Cleveland laboratory in February 1947. Analytical expressions are obtained for the wall contours of the supersonic part of the two-dimensional nozzle. An analytical expression for the straightening part of two-dimensional nozzles, in which source flow is considered to exist in the expanding part, has been derived by Kuno Foelsch of North American Aviation, Inc., but no method is given for creating such source flow. In order to present a complete discussion of two-dimensional nozzle design, the design of nozzle-wall contour for producing source flow in the expanding part of the nozzle and the design of the complementary straightening part are presented. A less complete treatment of this problem from a different point of view has been given by A. O. L. Atkin in a British report.

A working knowledge of the method of characteristics is desirable in order to understand and use the nozzle-design method. For this reason, the form of the method of characteristics most convenient for discussing the method of nozzle design considered is given in an appendix. A summary of the design equations and a sample nozzle design are included.

METHOD OF ANALYSIS

It will be demonstrated that when source flow is created entirely across the nozzle channel at any section, adjacent areas of the flow also have the properties of source flow. On this basis, analytical expressions are derived for the nozzle-wall coordinates required to create a specified source flow in the expanding part of the nozzle and to turn that flow into a uniform stream parallel to the nozzle axis in the straightening part with the desired Mach number. Only irrotational flows are considered in this analysis. The total temperature and the total pressure are constant throughout the flow. The flow adjacent to the nozzle walls is assumed to follow the wall contour at all times.

PROPERTIES OF SOURCE FLOW

In most conventional supersonic nozzles, source flow is approximated at the end of the expanding part of the nozzle. Because of the simple mathematical relations governing source flow, it is desirable to specify that perfect source flow exists at the end of the expanding part of the nozzle to obtain analytical expressions of simple form for the nozzle-wall coordinates.

The essential properties of two-dimensional source flow are illustrated in figure 2. In the supersonic part (solid lines),

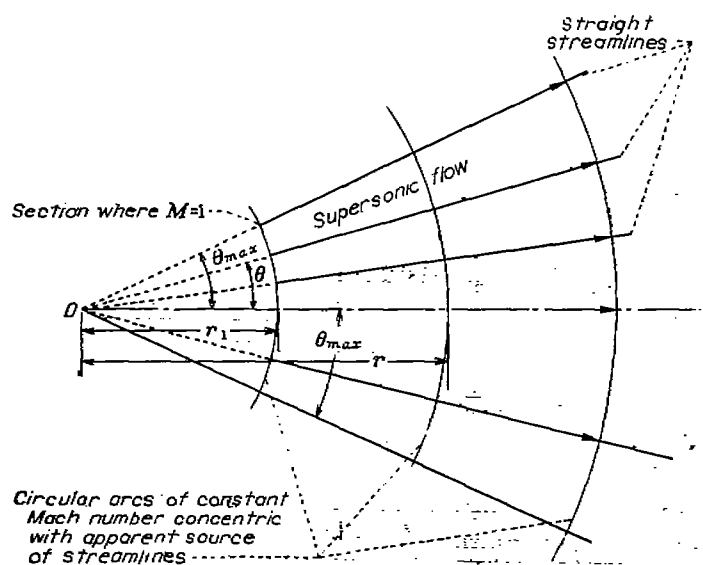


FIGURE 2.—Source flow.

streamlines are straight and appear to diverge from the apparent upstream source O. All stream tubes with the same included angle θ between bounding streamlines carry the same mass flow. From one-dimensional supersonic-flow theory, which applies to this type of flow because the flow is uniform on circular cylindrical surfaces concentric with the apparent source, the Mach number at points a distance r (fig. 2) from the apparent source is given by the following expression:

$$\frac{A_r}{A_1} = \frac{\theta r}{\theta r_1} = \frac{1}{M_r} \left(\frac{1 + \frac{\gamma-1}{2} M_r^2}{\frac{\gamma+1}{2}} \right)^{\frac{\gamma+1}{2(\gamma-1)}} = \frac{r}{r_1} \quad (1)$$

where A_r is the flow area per unit depth normal to the streamlines at a distance r from the source and A_1 is the corresponding flow area at $M=1$. (For convenience, all symbols are defined in appendix A.) The parameter r_1 is the distance from the apparent source to the arc at which the Mach number is unity, corresponding to the location of apparent throat of the source flow. The area of cross section normal to the flow at which $M=1$ is

$$A_1 = 2\theta_{\max} r_1$$

or

$$r_1 = \frac{A_1}{2\theta_{\max}}$$

Equation (1) then becomes

$$r = \frac{A_1}{2\theta_{\max}} \frac{1}{M_r} \left(\frac{1 + \frac{\gamma-1}{2} M_r^2}{\frac{\gamma+1}{2}} \right)^{\frac{\gamma+1}{2(\gamma-1)}} \quad (1a)$$

EXPANSION WAVES AND CHARACTERISTICS

According to the discussion in appendix B, changes in flow direction and Mach number in diverging channels are produced by a system of expansion waves originating at the channel walls. The change in flow direction due to an expansion wave from one channel wall is constant along Mach lines directed downstream of their point of contact with the channel wall where the wave originates. In the absence of expansion waves from the second wall, these Mach lines are straight and all the flow experiences the same change in direction and Mach number between the same two Mach lines in the expansion wave. If the flow enters the channel with uniform direction and Mach number, the flow direction and the Mach number are constant for the entire flow along these straight Mach lines in the expansion wave. The Mach number and the flow direction are the same as that of the flow moving adjacent to the channel wall at the point of contact with the Mach line. A number can be assigned to the Mach line that is equal to an expansive angular turn about a corner in a wall, bounding the flow, required to convert a sonic flow ($M=1$) to the same Mach number as that along the Mach line, according to the well-known Prandtl-Meyer theory (reference 2). Mach lines so numbered are called characteristics. The characteristics originating at the upper wall of the nozzle (fig. 3) are designated by (Ψ_+) and from the lower wall by (Ψ_-) . Each point in the flow is crossed by a (Ψ_+) and a (Ψ_-) characteristic corresponding to the two Mach lines through every point in a supersonic flow. The value of (Ψ_+) assigned to a characteristic represents the counterclockwise angular turning that would be experienced by the streamline coming from the left between the region where the flow is uniform with a Mach number of unity and the (Ψ_+) characteristic in the absence of the system of expansion waves designated by the (Ψ_-) characteristics. Similarly, the value of the (Ψ_-) characteristic represents the clockwise turning experienced by a streamline from the left between the region

and the value of the (Ψ_-) characteristic through B' (fig. 4) is

$$(\Psi_-)_{B'} = \frac{\Psi_I}{2} + \alpha \quad (4b)$$

Between the upper nozzle wall and the characteristic through I' (zone I, fig. 4), the (Ψ_+) characteristics are straight lines because the expansion waves from the upper wall are not crossed by any waves from the lower wall. (See appendix B.) Likewise, in zone II the (Ψ_-) characteristics are straight for corresponding reasons. In zone III expansion waves from the upper and lower walls overlap and the characteristics are curved.

The complete wave pattern for nozzles of the type considered is schematically shown in figure 3. The first expansion waves to leave the nozzle wall at points I and I' are bounded upstream by the $(\Psi_+)_I$ and $(\Psi_-)_{I'}$ characteristics, respectively. Because of the symmetry of the nozzle, these characteristics arrive at corresponding points E' and E on the opposite walls. Therefore, between points I and E no expansion waves are incident upon the nozzle walls. In the straight-walled part between sections $E-E'$ and $S-S'$, expansion waves are emitted having strength equal to the incident waves from the opposite wall. In order that no expansion waves be emitted from the portion of the wall between S and N (straightening part), the wall in this part of the nozzle is curved toward the nozzle axis. The curvature of the nozzle wall is the same as that assumed by the streamline moving along the wall under the influence of the incident expansion waves from the opposite wall. (See appendix B.) No waves are emitted by the wall between points S and N , therefore, and zones IV and V are traversed by one set of expansion waves whose characteristics are straight.

SOURCE FLOW IN NOZZLES

The nozzle-design method considered in this report is based upon establishing source flow at circular-arc section $E-E'$ (fig. 4). At this section the inclination of the wall to the axis has an assigned value α_E and the assigned Mach number of the flow is M_E . The choice of the values of α_E and M_E at section $E-E'$ is considered in the section "Design of complete nozzle." It will first be shown that if source flow exists at section $E-E'$ it exists everywhere in zone III. The flow between points in zone III is then related by equation (1a). This fact, together with the fact that the characteristics in zones I and II are straight, is the basis for establishing an analytical expression for the nozzle-wall contour producing the stipulated source flow at section $E-E'$.

The point of intersection of the straight line tangent to the nozzle wall at section $E-E'$ (fig. 4) and the nozzle axis represents the location O of the apparent source creating the source flow through section $E-E'$. At all points on section $E-E'$, the Mach number is constant. At a point on section $E-E'$ where the flow makes the angle θ with the axis, the following relations from equations (2) and (2a) apply:

$$\Psi_E = (\Psi_+) + (\Psi_-) = \lambda \tan^{-1} \frac{\sqrt{M_E^2 - 1}}{\lambda} - \tan^{-1} \sqrt{M_E^2 - 1} \quad (5)$$

where $\lambda = \sqrt{(\gamma+1)/(\gamma-1)}$

$$\theta = (\Psi_+) - (\Psi_-) \quad (5a)$$

At a point F on section $E-E'$ through which the flow makes the angle θ with the axis, from equations (5) and (5a),

$$(\Psi_+) = \frac{\Psi_E + \theta}{2} \quad (6)$$

and

$$(\Psi_-) = \frac{\Psi_E - \theta}{2} \quad (6a)$$

Inasmuch as source flow exists on section $E-E'$, θ is known at every point on the section and the complete system of characteristics can be specified on the section.

The flow in the neighborhood of point F on section $E-E'$ at which source flow is considered to be established is shown in detail in figure 5. It will be demonstrated that at point G , a distance dr from F toward the apparent source along the streamline through F , the streamline has the same direction as at F . Moreover, on the circular-arc section through

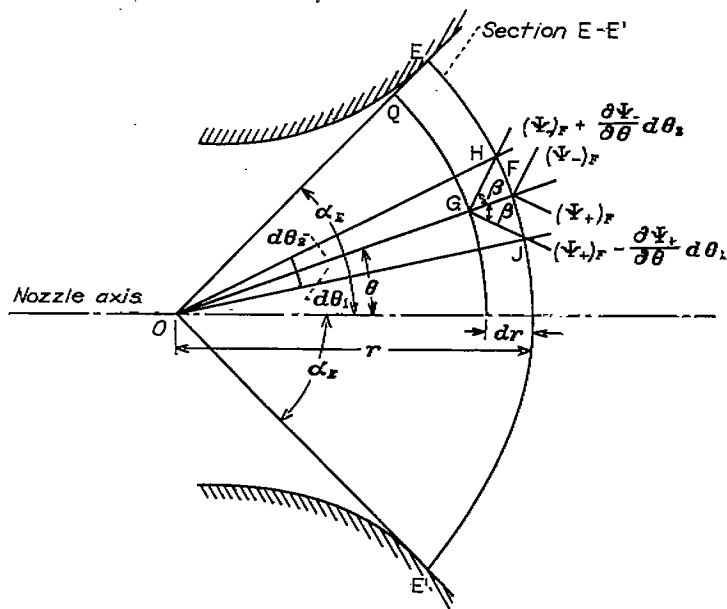


FIGURE 5.—Schematic representation of flow in neighborhood of section $E-E'$.

QG concentric with O , the Mach number is constant. Because the Mach number is constant on section $E-E'$, from equation (5), or (6) and (6a),

$$\frac{\partial(\Psi_+)}{\partial\theta} = -\frac{\partial(\Psi_-)}{\partial\theta} \quad (6b)$$

holds for all points on section $E-E'$. The (Ψ_+) and (Ψ_-) characteristics GJ and GH make the Mach angle β with the streamline through point F , so that the length of arcs HF and FJ are equal according to the equation

$$rd\theta_2 = HF = dr \tan \beta = FJ = rd\theta_1 \quad (7)$$

Therefore

$$d\theta_2 = d\theta_1 \quad (7a)$$

At point G

$$\begin{aligned} \theta_G = (\Psi_+)_G - (\Psi_-)_G &= \left[(\Psi_+)_F - \frac{\partial(\Psi_+)}{\partial\theta} d\theta_1 \right] - \left[(\Psi_-)_F + \frac{\partial(\Psi_-)}{\partial\theta} d\theta_2 \right] \\ &= (\Psi_+)_F - (\Psi_-)_F - \left[\frac{\partial(\Psi_+)}{\partial\theta} d\theta_1 + \frac{\partial(\Psi_-)}{\partial\theta} d\theta_2 \right] \end{aligned} \quad (7b)$$

From equation (4)

$$(\Psi_-)' = \frac{\Psi_I}{2}$$

and from equation (11c)

$$\theta = \Psi - \Psi_I \quad (11d)$$

and r is given by equation (11b).

The nozzle-wall coordinates of the expanding part can now be directly obtained from the following argument: Because zone I contains expansion waves from only the upper wall, a characteristic such as UV (fig. 6) in zone I is straight and the flow at every point on the line has the same Mach number and flow direction θ . (See appendix B.) The flow lines crossing each characteristic at any point in zone I make the same angle $\beta = \sin^{-1} \frac{1}{M}$ with the characteristic. Source flow exists on circular arc VW concentric with O and the Mach number is constant for all points on the arc. Point V is common to the arc VW and the Mach line UV and, inasmuch as there are no discontinuities in the flow, the Mach number is constant along the line UVW. Because the flow is considered to have constant total pressure and total temperature, the properties of the fluid, such as density, static pressure, static temperature, and flow speed, are constant along line UVW. The continuity condition for steady flow requires that the mass flow be the same across section E-E' and UVW. If source flow did exist in the entire wedge-shaped zone between the nozzle axis and the straight line OE, the Mach number of the flow across arc TV concentric with O would be the same as actually exists along VW or UV. The mass flow that crosses Mach line UV would cross arc TV with the same density and velocity. The area $l \sin \beta$ normal to the flow crossing Mach line UV must therefore be equal to the area normal to the assumed source flow crossing TV. As TV is the arc normal to the direction of the assumed source flow,

$$l \sin \beta = r(\alpha_E - \theta) \quad (12)$$

By means of the relation $\sin \beta = \frac{1}{M}$

$$l = Mr(\alpha_E - \theta) \quad (12a)$$

If X, Y and x, y are taken as the wall coordinates and the coordinates of the $(\Psi_-)'$ characteristic, respectively, then from figure 6

$$X = x - l \cos(\beta - \theta) = r \cos \theta - Mr(\alpha_E - \theta) \cos(\beta - \theta) \quad (13)$$

$$Y = y + l \sin(\beta - \theta) = r \sin \theta + Mr(\alpha_E - \theta) \sin(\beta - \theta) \quad (13a)$$

Negative values of X are possible.

All terms in equations (13) and (13a) are functions of M . These functions, taken from equations (11b) and (11d), are listed here for convenience:

$$r = \frac{A_t}{2\alpha_E M} \left(\frac{1 + \frac{\gamma-1}{2} M^2}{\frac{\gamma+1}{2}} \right)^{\frac{\gamma+1}{2(\gamma-1)}}$$

$$\theta = \lambda \tan^{-1} \frac{\sqrt{M^2 - 1}}{\lambda} - \tan^{-1} \sqrt{M^2 - 1} - \Psi_I$$

$$= \Psi - \Psi_I$$

$$\beta = \sin^{-1} \frac{1}{M}$$

Values for

$$r \left(\frac{2\alpha_E}{A_t} \right) = \frac{1}{M} \left(\frac{1 + \frac{\gamma-1}{2} M^2}{\frac{\gamma+1}{2}} \right)^{\frac{\gamma+1}{2(\gamma-1)}} = \frac{r}{r_1}$$

and

$$\theta + \Psi_I = \Psi = \lambda \tan^{-1} \frac{\sqrt{M^2 - 1}}{\lambda} - \tan^{-1} \sqrt{M^2 - 1}$$

are given in table I, column 4 and column 3, respectively.

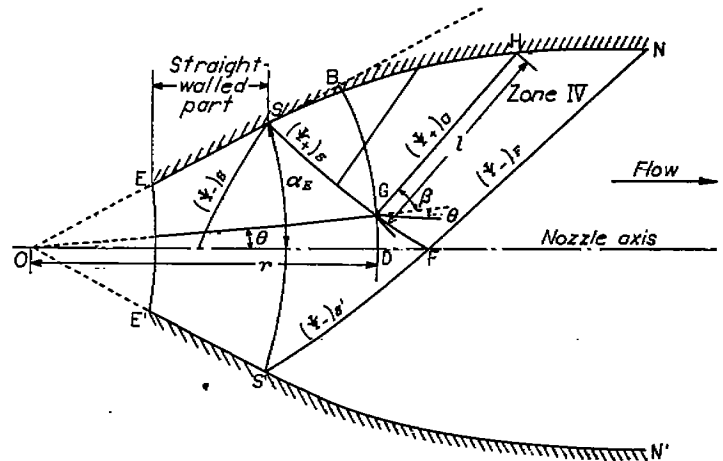


FIGURE 7.—Straightening part of nozzle.

The values of M used in equations (13) and (13a) range from M_I to M_E . The method of selecting α_E will be discussed in connection with over-all nozzle-design considerations. The values of M_I and M_E depend on the choice of α_E in a manner to be discussed subsequently.

Once source flow is established at section E-E' by nozzle walls shaped according to equations (13) and (13a), the source flow across the complete channel continues downstream of section E-E' as long as the nozzle walls are straight and have the inclination α_E with the nozzle axis. Downstream of section S-S', the end of the straight-walled part (fig. 7), the source-flow zone extends from the axis to the $(\Psi_+)_S$ characteristic in the upper half of the nozzle and the $(\Psi_-)_{S'}$ characteristic in the lower half of the nozzle. The proof of this fact is similar to that given previously for the zone immediately upstream of section E-E' (fig. 5).

VALUE OF Ψ_I

If the uniform parallel flow across section 1-1' (fig. 4) were at a Mach number of unity, both limiting Mach lines, or characteristics, 1'E and 1'E' would leave their respective nozzle walls with direction normal to the nozzle axis and would arrive at the opposite wall without displacement downstream. In this case the length of the expanding section of the nozzle would be zero.

The minimum value of Ψ_I required to obtain a length of nozzle sufficient to permit an assigned value of α_E at section E-E' is obtained from the physical requirement that the value of M must always increase with increasing value of X , the nozzle-wall coordinate given in equation (13). The minimum value of M_I , corresponding to the minimum value of Ψ_I , (equation (2)) is obtained from

$$\alpha_E = \frac{(M_I^2 - 1)^{3/2}}{0.6M_I^4} \quad (14)$$

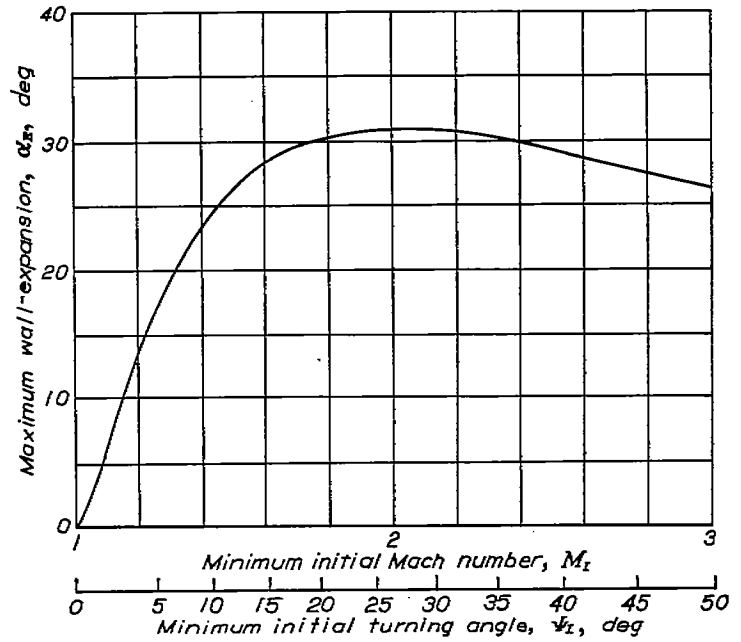
for $\gamma=1.400$. The development of this equation is given in appendix C. Values of M_I less than those given by equation (14) give negative values of $\frac{\partial X}{\partial M}$ in the neighborhood of section 1-1'. A plot of equation (14) is given in figure 8.

The highest value α_E can have (fig. 8) is about 31° , corresponding to a value of $M_I=2$. Source flow cannot be produced in nozzles with α_E greater than 31° . The corresponding values of Ψ_I given by equation (14) lie between 0 and Ψ_I corresponding to $M_I=2$. The values of Ψ_I plotted in figure 8 are minimum values. Over-all design considerations or ease of computation may suggest values of Ψ_I greater than these minimum values. If a higher value is chosen for Ψ_I , the corresponding value of α_E required to obtain the desired value of M_I is computed in a manner to be considered in the section "Design of Complete Nozzle."

WALL CONTOUR OF STRAIGHTENING PART OF NOZZLE

The straightening part of the nozzles considered converts a supersonic source flow into a uniform flow parallel to the nozzle axis. Consider a supersonic source flow at circular-arc section S-S' concentric with apparent source (fig. 7). Circular-arc section S-S' may be coincident with section E-E' or may be a section downstream of section E-E'. If it is downstream, source flow exists across the entire straight-walled channel of the nozzle between sections E-E' and S-S'. Because the nozzle-wall curvature between points S and N will influence the flow only downstream of the forward Mach line through point S ($(\Psi_+)_s$ characteristic), the source flow ends at the $(\Psi_+)_s$ characteristic upstream of point F.

The straightening part of the nozzle is designed on the principle that the wall contour is shaped to conform to the curvature of the streamline adjacent to the wall that is turned by the incident expansion wave from the opposite wall. No emission of either expansion or compression waves occurs from the wall so shaped. This point is discussed in

FIGURE 8.—Maximum wall-expansion angle α_E . $\gamma=1.400$.

appendix B. The $(\Psi_+)_s$ characteristic therefore represents the downstream limit of all expansion waves emanating from the upper nozzle wall. The zone enclosed by the lines joining the points SFN contains waves that originate at the lower nozzle wall only. The (Ψ_-) characteristics in this zone are therefore straight. (See appendix B.)

The equation of the limiting characteristic $(\Psi_+)_s$ is obtained by making use of the fact that source flow exists in the adjacent area upstream of the $(\Psi_+)_s$ characteristic. If x and y are the coordinates parallel and normal to the nozzle axis, respectively, of the $(\Psi_+)_s$ characteristic with the origin taken at the apparent source, then

$$\begin{aligned} x &= r \cos \theta \\ y &= r \sin \theta \end{aligned} \quad (15)$$

where r is given as a function of M by equation (11b). By the same reasoning used to obtain equation (11d), θ is obtained as

$$\begin{aligned} \theta &= (\Psi_+)_s - (\Psi_-) = -[(\Psi_+)_s + (\Psi_-)] + 2(\Psi_+)_s = 2(\Psi_+)_s - \Psi \\ &= 2(\Psi_+)_s - \lambda \tan^{-1} \frac{\sqrt{M^2 - 1}}{\lambda} + \tan^{-1} \sqrt{M^2 - 1} \end{aligned} \quad (16)$$

The values of M range from M_s to M_f . The value of $(\Psi_+)_s$ is obtained from the observation that a streamline along the nozzle axis arriving at point F (fig. 7) will have crossed all expansion waves emanating from both walls and will therefore be at the final flow Mach number M_f corresponding to a total turning angle Ψ_f . Because the inclination of the flow to the axis is zero at point F, values of (Ψ_+) and (Ψ_-) of the characteristics through point F are related by the equation

$$\theta = (\Psi_+)_F - (\Psi_-)_F = 0$$

Moreover, the (Ψ_+) and (Ψ_-) characteristics through F are the limiting characteristics $(\Psi_+)_S$ and $(\Psi_-)_{S'}$, respectively; therefore

$$(\Psi_+)_F = (\Psi_+)_S = (\Psi_-)_{S'} = (\Psi_-)_F$$

Because in a symmetrical nozzle $(\Psi_+)_S = (\Psi_-)_{S'}$, and

$$\Psi_F = (\Psi_+)_F + (\Psi_-)_F = 2(\Psi_+)_F = 2(\Psi_+)_S$$

$$(\Psi_+)_S = \frac{\Psi_F}{2} \quad (16a)$$

From the fact that the flow through point F is at the final Mach number M_f , $\Psi_F = \Psi_f$ and equation (16) can then be written

$$\theta = \Psi_f - \Psi = \Psi_f - \lambda \tan^{-1} \frac{\sqrt{M^2 - 1}}{\lambda} + \tan^{-1} \sqrt{M^2 - 1} \quad (16b)$$

where M has values between M_s and M_f . The value of M_s corresponds by equation (2) to $\Psi_s = (\Psi_+)_S + (\Psi_-)_S$. Because the flow direction at point S makes the angle α_s with the nozzle axis (fig. 7)

$$(\Psi_+)_S - (\Psi_-)_S = \alpha_s$$

Therefore, from equation (16a)

$$\Psi_s = 2(\Psi_+)_S - \alpha_s = \Psi_f - \alpha_s \quad (16c)$$

The coordinates X, Y of the nozzle wall for the straightening part are obtained in a manner similar to those for the expanding section. A characteristic (such as GH in zone IV (fig. 7)), included in area SFN is straight and the Mach number is constant along the characteristic. (See appendix B.) Consequently, the flow direction, pressure, temperature, and velocity are constant along such characteristics. Along the circular arc GD, source flow exists and the Mach number, pressure, and temperature are constant. Only the flow direction varies along GD. As point G is common to GH and arc GD, the physical properties of the fluid and the flow speed along GD are the same as along GH. The area of flow normal to the streamlines along HGD is

$$A = r\theta + l \sin \beta \quad (17)$$

If source flow had existed downstream of section S-S', as it would have if the nozzle walls had continued downstream straight through S, then the mass flow across arc BGD would have the same value as across HGD. The fluid would also have had the same pressure, temperature, density, and flow Mach number as actually exists on arc GD, which does support source flow. The area normal to the flow across BGD would therefore be the same as for the flow that does cross HGD and from equation (17)

$$r\alpha_s = r\theta + l \sin \beta \quad (17a)$$

$$\text{As } \sin \beta = \frac{1}{M}$$

$$l = Mr(\alpha_s - \theta) \quad (17b)$$

Therefore, if X, Y and x, y are the nozzle-wall coordinates of the straightening part and the $(\Psi_+)_S$ characteristic, respectively, then

$$X = x + l \cos(\theta + \beta) = r \cos \theta + Mr(\alpha_s - \theta) \cos(\theta + \beta) \quad (18)$$

$$Y = y + l \sin(\theta + \beta) = r \sin \theta + Mr(\alpha_s - \theta) \sin(\theta + \beta) \quad (18a)$$

The values of r are obtained from equation (11b) and are tabulated in table I, column 4. The value of θ is obtained from $\Psi_f - \theta$ (given in table I, column 3) corresponding to the value of M for which the point (X, Y) (equations (18) and (18a)) is being obtained. The value of Ψ_f corresponding to M_f , the final Mach number of the nozzle, is also obtained from table I, column 3. The value of M to be used in equations (18) and (18a) ranges from M_s to M_f .

DESIGN OF COMPLETE NOZZLE

Supersonic nozzles are generally specified in terms of the cross-sectional area of final uniform flow A_f and the final Mach number M_f . The nozzle-throat area is obtained by the one-dimensional-flow equation

$$\frac{A_f}{A_t} = \frac{1}{M_f} \left(\frac{1 + \frac{\gamma-1}{2} M_f^2}{\frac{\gamma+1}{2}} \right)^{\frac{\gamma+1}{2(\gamma-1)}}$$

for which values are tabulated in table I, column 4.

NOZZLE WITHOUT STRAIGHT-WALLED PART

The shortest nozzles that may be designed by the method reported are those without a straight-walled part between sections E-E' and S-S'. The straightening part immediately follows the expanding part. For a given value of M_f and given final Mach number M_f , the value of α_s is fixed by the following consideration: Because α_s is the angle through which the nozzle wall turns between section I-I' and section E-E' (fig. 3), then

$$(\Psi_+)_E - (\Psi_+)_I = \alpha_s \quad (19)$$

By equation (4)

$$\alpha_s = (\Psi_+)_E - \frac{\Psi_f}{2} \quad (19a)$$

The value of (Ψ_+) remains constant at $(\Psi_+)_E$ downstream of the $(\Psi_+)_E$ characteristic because no additional waves are emitted from the upper wall of the shortest nozzle (fig. 9). The value of (Ψ_-) likewise remains constant at $(\Psi_-)_{E'}$ downstream of the $(\Psi_-)_{E'}$ characteristic. At the end of the nozzle, where the flow is parallel to the nozzle axis with a uniform Mach number M_f ,

$$\theta = 0 = (\Psi_+)_E - (\Psi_-)_{E'}$$

$$\Psi_f = (\Psi_+)_E + (\Psi_-)_{E'} = 2(\Psi_+)_E = 2(\Psi_-)_{E'} \quad (19b)$$

From equation (19a), therefore

$$\alpha_s = \frac{\Psi_f - \Psi_f}{2} \quad (19c)$$

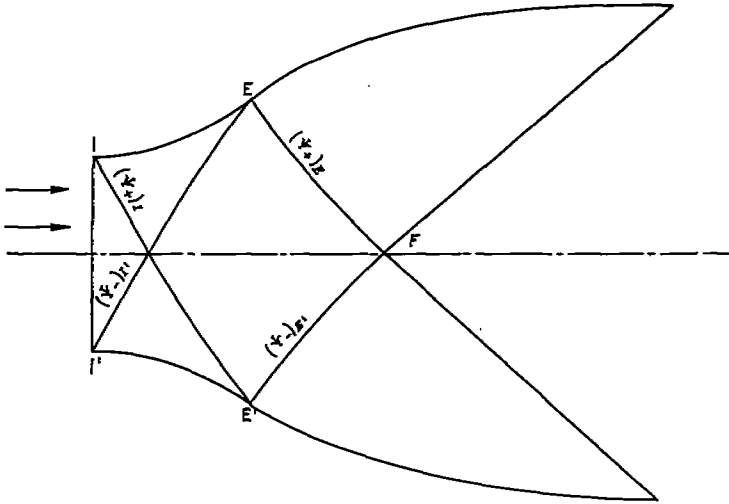


FIGURE 9.—Limiting characteristics in nozzle without straight-walled part.

The angle α_E is always less than one-half the equivalent turning angle Ψ_I required to obtain the final Mach number M_f .

Considerations of nozzle construction or flow stability may suggest a desirable value of α_E . Then Ψ_I is given by equation (19c) for a nozzle of given final Mach number M_f . The value of α_E chosen must correspond to a value of Ψ_I by equation (19c) that is equal to or greater than the minimum Ψ_I computed by equation (14) for the same value of α_E . (See fig. 8.) A small saving in length of nozzle is made if a value of α_E and the corresponding value of Ψ_I are obtained from the simultaneous solution of equations (14) and (19c). These values are given in a plot of α_E and the corresponding minimum value of Ψ_I required is given in figure 10 for a range of values of M_f from 1 to 10. In the high range of values of final Mach number M_f , Ψ_I exceeds α_E . If large values of Ψ_I are undesirable, lower values may be used in conjunction with a straight-walled part of the nozzle as discussed in the next section.

NOZZLE WITH STRAIGHT-WALLED PARTS

If nozzles are desired having known values of α_E and Ψ_I less than those given by equations (14) and (19c) (fig. 10), then a straight-walled portion of the nozzle is required downstream of section E-E' to obtain the desired value of M_f . The length of the required straight-walled part is obtained as follows: According to equation (11b), which applies to source flow, the axial distance between circular-arc sections E-E' and S-S' is

$$r_S - r_E = \frac{A_t}{2\alpha_E} \left[\frac{1}{M_S} \left(\frac{1 + \frac{\gamma-1}{2} M_S^2}{\frac{\gamma+1}{2}} \right)^{\frac{\gamma+1}{2(\gamma-1)}} - \frac{1}{M_E} \left(\frac{1 + \frac{\gamma-1}{2} M_E^2}{\frac{\gamma+1}{2}} \right)^{\frac{\gamma+1}{2(\gamma-1)}} \right] \quad (20)$$

The values of M_E and M_S are obtained from the corresponding values of Ψ_E and Ψ_S evaluated in the following manner:

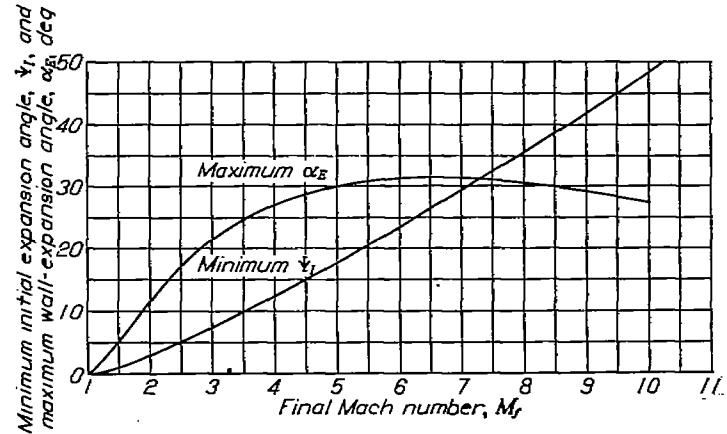
The expression for Ψ_E is obtained from equations (4) and (4a) and figure 4 as

$$\Psi_E = (\Psi_+)_E + (\Psi_-)_{I'} = \frac{\Psi_I}{2} + \alpha_E + \frac{\Psi_I}{2} = \Psi_I + \alpha_E \quad (20a)$$

From equation (16c)

$$\Psi_S = \Psi_I - \alpha_E \quad (20b)$$

The values of Ψ_E and Ψ_S from equations (20a) and (20b) provide by means of table I, columns 1 and 3, the corresponding value of M_E and M_S required in equation (20). The values of r_S and r_E likewise can be obtained from table I, column 4. The only theoretical condition on the choice of

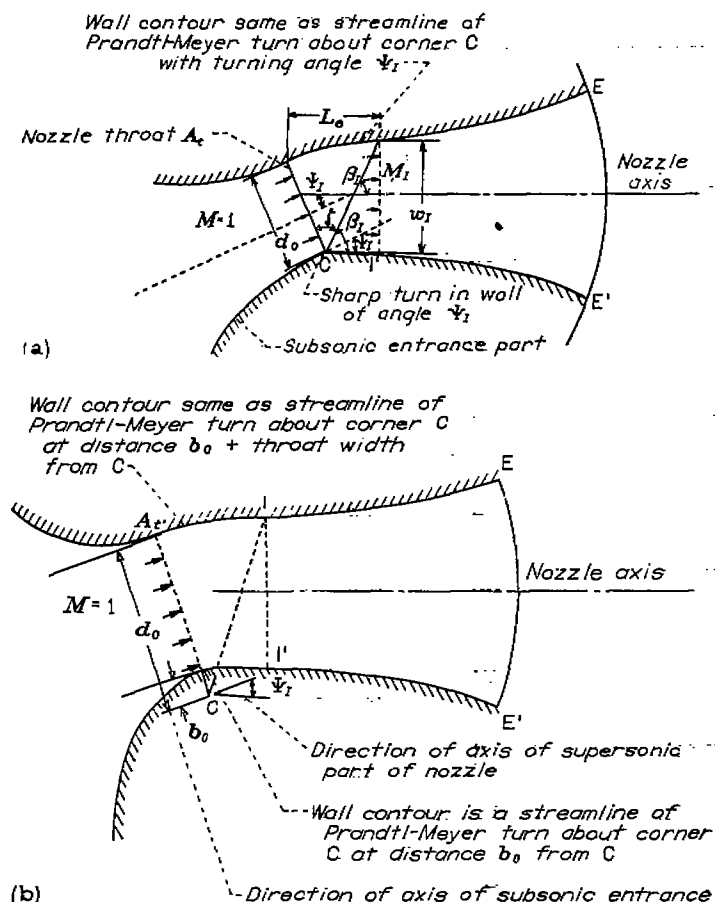
FIGURE 10.—Minimum initial turning angle Ψ_I and maximum wall-expansion angle α_E . $\gamma=1.400$.

Ψ_I and α_E is that Ψ_I shall not be less than the value given by equation (14) (fig. 8) for the value of α_E chosen (less than 31°).

DESIGN OF INITIAL EXPANSION PART

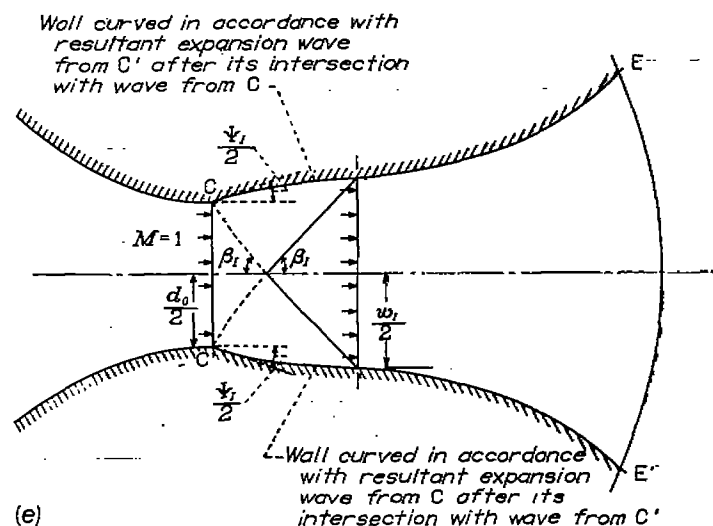
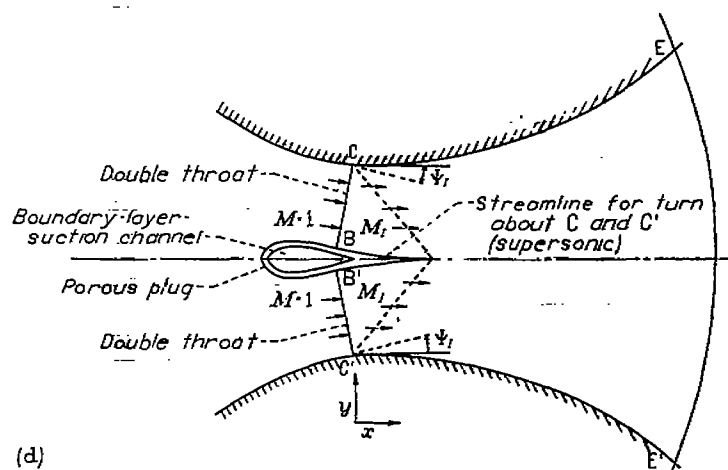
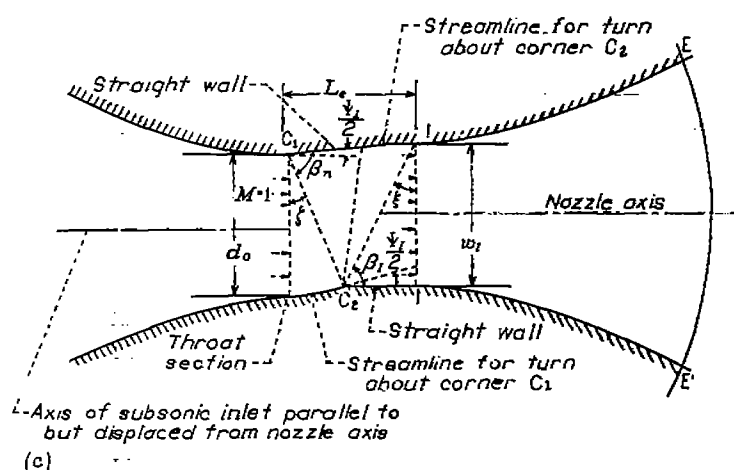
Exact nozzle-wall contours for converting a uniform flow at Mach number unity to a uniform supersonic flow at Mach number M_f can be obtained by shaping the nozzle walls to conform to the streamlines corresponding to the turning of a sonic flow about a corner according to Prandtl-Meyer theory. (Complete nozzles built according to this method have excessive length for high final Mach numbers. This length is undesirable if thick boundary layers on the nozzle walls are to be avoided.)

Four applications of the use of the solution for the turn about a corner to obtain the wall coordinate of the initial expansion part are illustrated in figure 11. In figure 11 (a) is shown the subsonic entrance part, the nozzle throat, the initial expansion part, and the expanding part of the nozzle. The lower wall of the initial expansion part is a sharp corner at C with an angle equal to Ψ_1 . The upper wall has the contour of a streamline of the flow around the sharp corner. In figure 11 (b) is illustrated the same type of initial expansion part in which the sharp corner at C of figure 11 (a) is replaced by a streamline of the flow around the sharp corner. In the arrangements of both figures 11 (a) and 11 (b), the axis of the subsonic entrance makes the angle Ψ_1 with the axis of the supersonic part of the nozzle. The axis of the subsonic inlet can be made parallel to, but offset from, the axis of the supersonic part of the nozzle by producing the initial expansion of the flow by means of a counterclockwise and clockwise turning of the flow about a corner at the upper wall (point C₁, fig. 11 (c)) and the lower wall (point C₂) each of angle $\Psi_1/2$. As in the case shown in figure 11 (b), the



(b) Upper and lower wall with contour of Prandtl-Meyer turn about corner.

FIGURE 11.—Methods of designing initial expansion part of nozzle.



(c) Initial expansion produced by corner at each wall.

(d) Initial expansion involving use of plug.

(e) Initial expansion produced by short nozzle at throat.

FIGURE 11.—Concluded. Methods of designing initial expansion part of nozzle.

corners at C_1 and C_2 can be replaced by streamlines. The arrangement illustrated in figure 11 (d) uses a plug whose contours downstream of the throat are shaped to conform to streamlines for the flow around the corners C and C' on the upper and lower walls, respectively. The turning angle at C and C' is Ψ_I degrees. The initial expansion of the flow is, in effect, accomplished by two separate initial expansion parts in parallel. The axis of the subsonic entrance is in line with the axis of the supersonic part of the nozzle.

An alternative form of the arrangement of figure 11 (d) is shown in figure 11 (e). No plug is required in this initial expansion part. The expansion waves arising at the turns at C and C' are intercepted without further remission by the opposite walls. As all the streamlines cross the expansion waves from both the upper and lower wall, the turning angles at C and C' are $\Psi_I/2$. The wall contours of the arrangement shown in figure 11 (e) are not streamlines of a Prandtl-Meyer turn about a corner but must be obtained by the standard graphical method to be discussed.

The expressions for the coordinates of the wall contour in which the initial turning of the flow is produced are now

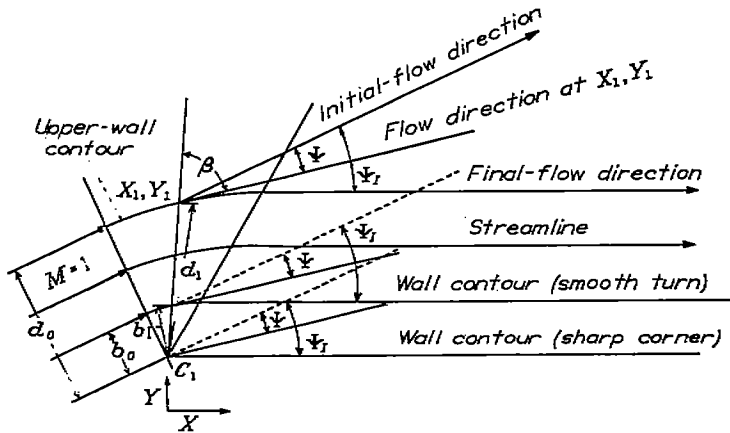


FIGURE 12.—Two-dimensional supersonic flow about corner.

obtained. In figure 12 is shown the supersonic flow about the corner of a two-dimensional wall in a supersonic flow of infinite extent. According to Prandtl-Meyer theory, the Mach number of the flow is constant along radial lines from the corner and all flow lines crossing a given radial line are parallel at the radial line. For a flow line a distance d_1 from the corner C_1 along a radial line, the total flow area normal to the flow, A_s , is $d_1 \sin \beta$. From the geometrical relation shown in figure 12, the coordinates of a given streamline (wall coordinates) are

$$X_1 = d_1 \cos (\beta + \Psi_I - \Psi) \quad (21)$$

$$Y_1 = d_1 \sin (\beta + \Psi_I - \Psi) \quad (21a)$$

where $\beta = \sin^{-1} \frac{1}{M}$ ($1 \leq M \leq M_I$). The value of d_1 is obtained from the one-dimensional flow relation

$$\frac{A_s}{A_t} = \frac{d_1 \sin \beta}{d_0} = \frac{d_1}{d_0} = \frac{1}{M} \left(\frac{1 + \frac{\gamma-1}{2} M^2}{\frac{\gamma+1}{2}} \right)^{\frac{\gamma+1}{2(\gamma-1)}}$$

$$d_1 = d_0 \left(\frac{1 + \frac{\gamma-1}{2} M^2}{\frac{\gamma+1}{2}} \right)^{\frac{\gamma+1}{2(\gamma-1)}} \quad (21b)$$

When the short wall of the initial expansion part is a sharp corner, then d_0 is equal to the width of the nozzle throat. If both walls in the initial turning portion of the nozzle are to conform to streamlines as illustrated in figure 11 (b), the throat width is given by $d_0 - b_0$. The coordinates of the long wall are given by equations (21) and (21a) and of the short wall by the same equation with b_1 and b_0 substituted for d_1 and d_0 , respectively, in equations (21), (21a), and (21b). The values of d/d_0 are given in table I, column 5.

When the initial expansion to M_I is accomplished in two steps, as shown in figure 11 (c), the coordinates of the walls of the first part are given by equations (21) and (21a) with Ψ_I replaced by $\Psi_I/2$. The coordinates of the wall of the second section about point C_2 are obtained from the geometric relations illustrated in figure 13. The angle between the flow direction at R and at G , where the flow direction is parallel to the nozzle walls, is $\Psi_I - \Psi$. If D is a point on the wall opposite to the location of corner C_2 and d_2 is the variable length C_2D , then the coordinates of the wall are

$$X_2 = d_2 \cos (\beta + \Psi_I - \Psi) \quad (22)$$

$$Y_2 = d_2 \sin (\beta + \Psi_I - \Psi) \quad (22a)$$

The coordinate axes at C_2 are turned at an angle $\Psi_I/2$ with respect to the axes at C_1 . The value of M ranges from M_* to M_I , where M_* corresponds to $\Psi_I/2$, or

$$\frac{\Psi_I}{2} \leq \Psi \leq \Psi_I$$

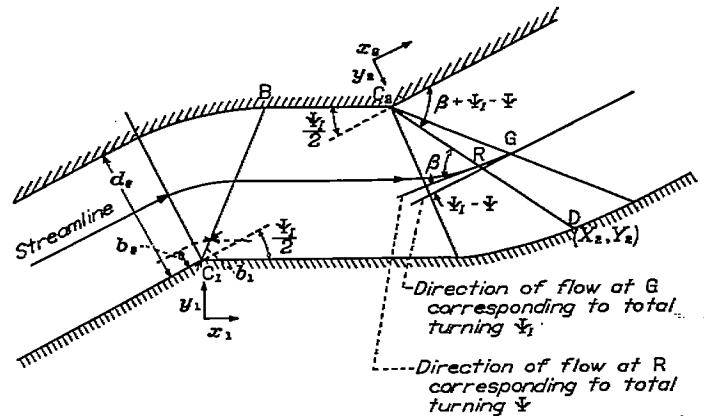


FIGURE 13.—Double initial turn, sharp corners.

Moreover,

$$d_2 = d_0 \left(\frac{1 + \frac{\gamma-1}{2} M^2}{\frac{\gamma+1}{2}} \right)^{\frac{\gamma+1}{2(\gamma-1)}} \quad (22b)$$

(from equation (21b)). Values of d_2/d_0 , shown as d/d_0 , are given in table I, column 5. Point C_2 can be coincident with point B (fig. 13).

If the coordinates of the walls with smooth turns (fig. 14) are desired in place of the sharp turns at C_1 and C_2 , they are obtained as before with b_1 , b_2 , and b_0 substituted for d_1 , d_2 , and d_0 , respectively, in equations (21) to (22a). The nozzle-throat width is then $d_0 - b_0$.

When a plug is used in the initial expansion part of the nozzle, as in figure 11(d), each wall has a turn equal to Ψ_I ; each turn influences the flow between the corresponding wall and the plug. The coordinates of the plug (fig. 11 (d)) downstream of the throat are given by equations (21) and (21a), in which d_0 is now the distance from the wall to the plug at the throat section CB. Smooth turns can be substituted for the corners at C by the method discussed in connection with figure 11 (b). Boundary-layer development on the plug may produce an undesirable wake. This condition may be alleviated by the boundary-layer-removal arrangements illustrated in figure 11 (d).

A graphical method for obtaining wall contours for the initial expansion corresponding to the configuration shown in figure 11(e) is illustrated in figure 15. The system of (Ψ_+) and (Ψ_-) characteristics emanating from the corners C and C' are curved in zone I to account for the effect of one

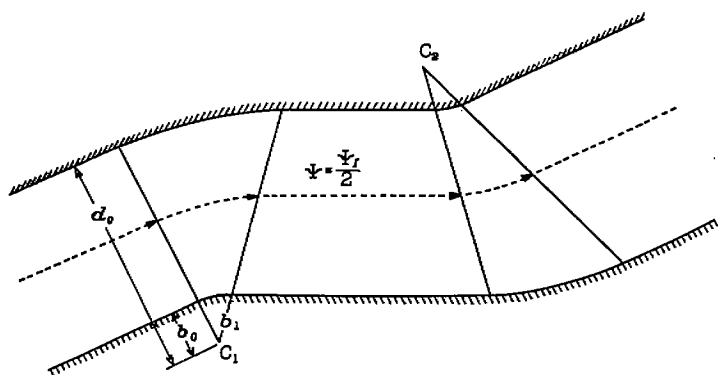


FIGURE 14.—Double initial turn, smooth turns.

set of expansion waves on the other in accordance with the discussion of appendix B. In zones II and III, the characteristics are straight because the nozzle walls are curved to prevent emission of waves downstream of points C and C' . Because all expansion waves from C and C' remain upstream of the (Ψ_+) and (Ψ_-) characteristics equal to $\Psi_I/2$, (Ψ_+) is constant everywhere in zone II at a value of $\Psi_I/2$. In zone III, (Ψ_-) is likewise constant everywhere at $\Psi_I/2$. If M_I represents the Mach number of the flow at section I-I'

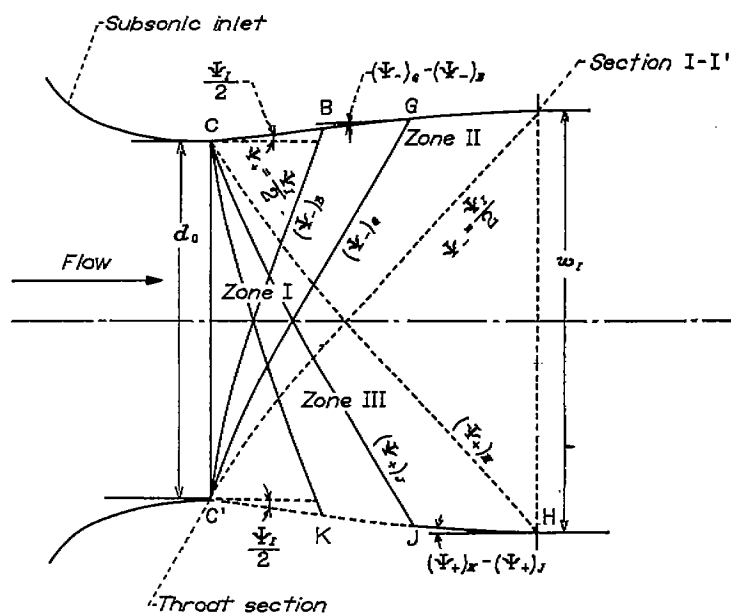


FIGURE 15.—System of characteristics for initial expansion part.

(fig. 15), then the width of the nozzle at section I-I' is obtained from the one-dimensional supersonic-flow relation

$$\frac{w_I}{d_0} = \frac{1}{M_I} \left(\frac{1 + \frac{\gamma-1}{2} M_I^2}{\frac{\gamma+1}{2}} \right)^{\frac{\gamma+1}{2(\gamma-1)}} \quad (23)$$

Values of the right side of equation (23) are given in table I, column 4.

Because the change in wall contour between points B and G (fig. 15) is made to conform to the curvature of the adjacent streamlines produced by the incident expansion waves, the change in wall angle α between B and G on the upper wall (zone II), is

$$\Delta\alpha = \Delta\theta = \theta_G - \theta_B = (\Psi_+)_G - (\Psi_-)_G - (\Psi_+)_B + (\Psi_-)_B$$

or, because $(\Psi_+)_G = (\Psi_+)_B = \frac{\Psi_I}{2}$,

$$-\Delta\alpha = (\Psi_-)_G - (\Psi_-)_B \quad (23a)$$

Similarly, on the lower wall (zone III),

$$-\Delta\alpha = (\Psi_+)_H - (\Psi_+)_J \quad (23b)$$

Beginning the graphical layout of the walls from section I-I', which has the calculated width w_I , in the manner shown at the lower wall (fig. 15), is advisable. This procedure insures that the ratio of the area at section I-I' to the throat section is correct and gives the desired value of M_I . The line HJ is drawn, making the angle $\Delta\alpha$ with the nozzle axis as determined by equation (23b). The line JK is drawn likewise, making the angle $\Delta\alpha$ with line HJ as determined from equation (23b) with K and J substituted for J and H, respectively. The polygon obtained by the method just described is replaced by a smooth curve through the vertices of the polygon.

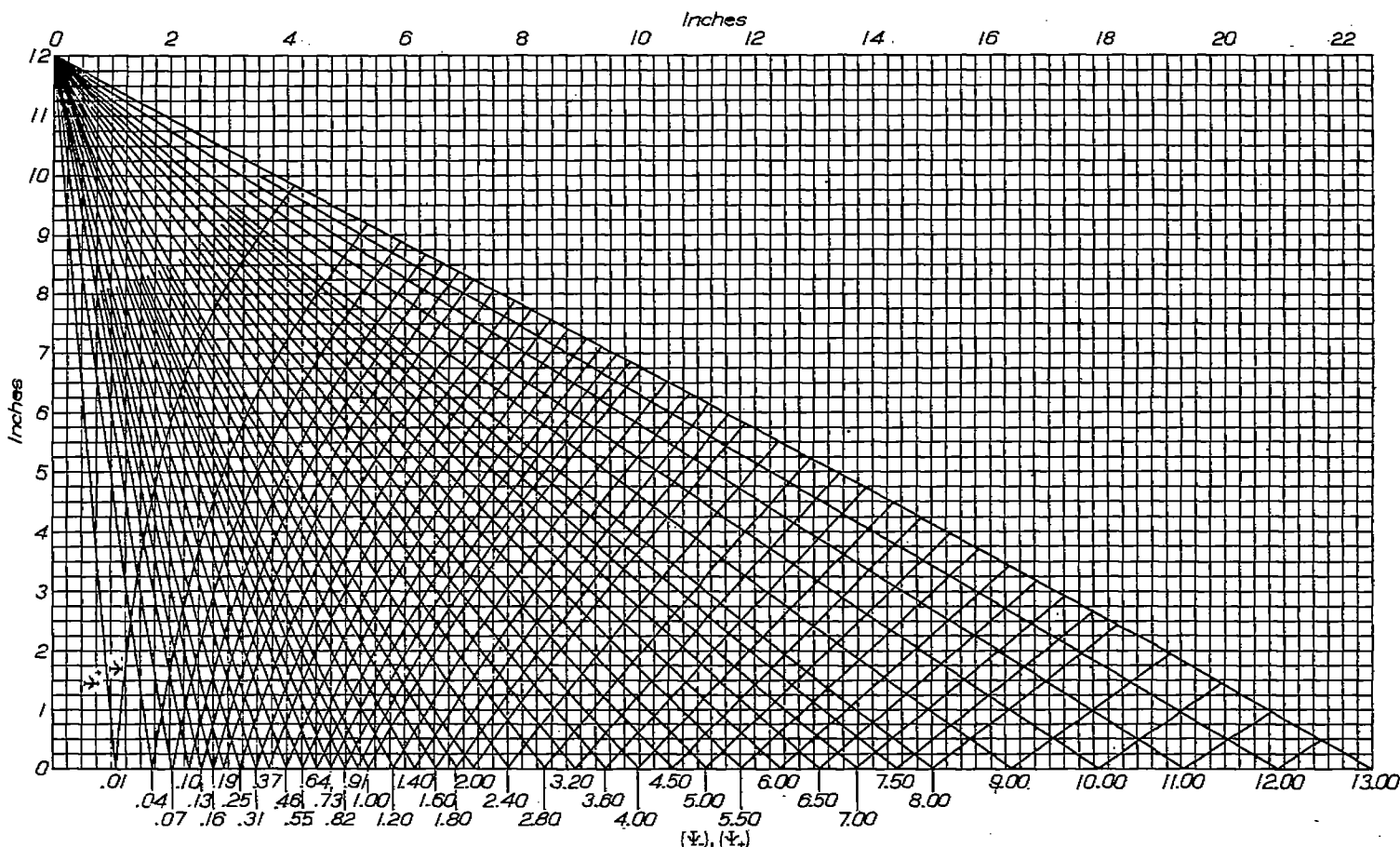


FIGURE 16.—System of characteristics for sharp-cornered throat. Maximum Mach number, 1.915.

(A 23.5- by 13.3-in. print of this chart is available on request from NACA.)

The system of characteristics for zone I of the initial expansion part of nozzles having values of M_f up to 1.536, which corresponds to an initial turning angle of 13° , is reproduced in figure 16. The zone I characteristics for an initial expansion part of equivalent angle Ψ_f are obtained by selecting all (Ψ_+) and (Ψ_-) characteristics having values equal to and less than $\Psi_f/2$. The zone II characteristics are obtained by continuing the set of (Ψ_-) characteristics as straight lines in the direction of the tangent to the characteristics at their point of intersection with the (Ψ_+) characteristic equal to $\Psi_f/2$. The zone III characteristics are obtained by continuing the set of (Ψ_+) characteristics as straight lines in the direction of the tangents to the characteristics at their intersection points with the (Ψ_-) characteristic equal to $\Psi_f/2$. A plot similar to that given in figure 15 results. Because the wall contour is determined by the zone II and zone III characteristics, the zone I characteristics need not be plotted. From zone I is obtained the direction and the coordinates of the zone II and zone III characteristics at the point of contact with the limiting (Ψ_+) and (Ψ_-) characteristics equal to $\Psi_f/2$. The direction and the coordinates of the characteristics can be obtained from the coordinate system given in figure 16. Tracings from figure 16 will be inaccurate because of the distortion of the figure during reproduction. The system of characteristics is given for a nozzle having a throat width of 24 inches.

The coordinates of the characteristics for nozzles having a different throat width A_t are obtained by multiplying all coordinates given in figure 16 by $A_t/24$. The slopes of the characteristics remain unaltered.

ESTIMATION OF NOZZLE LENGTH

The length of the supersonic part of the nozzle (fig. 17) is

$$L = X_f - X_i + L_e \quad (24)$$

As X_f is the coordinate of the downstream end of the nozzle where M is equal to M_f , its value is given by equation (18) with $\theta = 0$

$$X_f = r_f (1 + M_f \alpha_E \cos \beta_f) \quad (24a)$$

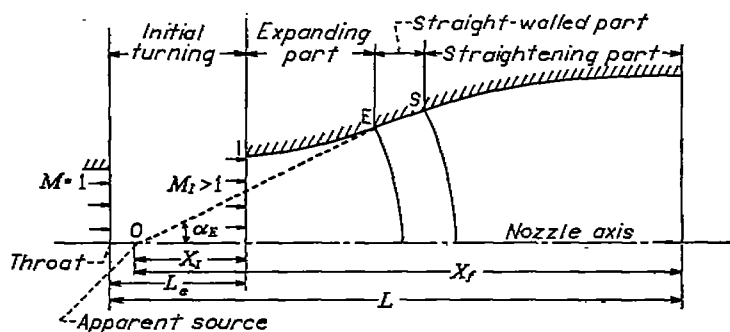


FIGURE 17.—Designation of lengths of nozzle parts.

where r_I and β_I are obtained from table I with $M=M_I$. The value of X_I , given by equation (13), corresponds to the coordinate of section 1-1' where M equals M_I and $\theta=0$

$$X_I = r_I (1 - M_I \alpha_E \cos \beta_I) \quad (24b)$$

Negative values of X_I are possible.

The length of the initial expansion part L_e (measured along the nozzle wall) is generally less than 10 percent of the total length of the nozzle. The following approximate expressions for L_e will in general suffice:

1. For one turn about a corner (fig. 11 (a)),

$$\begin{aligned} L_e &\approx d_0 \tan \zeta = d_0 \tan (90^\circ + \Psi_I - \beta_I) \\ L_e &\approx d_0 \cot (\beta_I - \Psi_I) \end{aligned} \quad (24c)$$

where Ψ_I is obtained from table I for $M=M_I$.

2. For two turns in succession about a corner at each wall (fig. 11 (c)),

$$\begin{aligned} L_e &\approx d_0 \tan \zeta + w_I \tan \xi = d_0 \tan (90^\circ + \frac{\Psi_I}{2} - \beta_n) + \\ &w_I \tan (90^\circ - \beta_I) = d_0 \cot (\beta_n - \frac{\Psi_I}{2}) + w_I \cot \beta_I \end{aligned} \quad (24d)$$

where $\beta_n = \sin^{-1} \frac{1}{M_n}$, and M_n corresponds to $\Psi_I/2$ from table II.

3. For the nozzle with the plug (fig. 11 (d)), the value of L_e is 0.

4. For the short nozzle at the throat (fig. 11 (e)), the axial length of the corresponding initial expansion part is approximately

$$L_e \approx \frac{d_0 + w_I}{2} \cot \beta_I \quad (24e)$$

REMARKS ON APPLICATION OF DESIGN METHOD

Mathematical expressions for the wall coordinates of supersonic nozzles in which source flow is developed are

valid for values of α_E equal to or less than 31° . The assumption that the flow follows the nozzle wall for values of α_E up to 31° must be verified by experiment. The use of sharp corners at the initial expansion part must be checked as well. Until this check is made, α_E may well be restricted to known safe values and smooth turns used instead of sharp corners. Because of the favorable pressure gradient in the expansion part of the nozzle, however, the flow will probably follow the nozzle wall for all values of α_E permitted by the theory. Satisfactory flow around sharp corners is also likely for the same reason.

A sample calculation is given in table III of all the design parameters and typical wall coordinates for two nozzles having a final Mach number of $M=3.50$ and a final width of 10 inches. One nozzle has an initial expansion part consisting of one turn about a sharp corner and belongs to the class of shortest nozzles. The other nozzle has an initial turning part consisting of two turns about sharp corners and contains a straight-walled part.

No account was taken of the effect of boundary-layer growth on the walls on the nozzle flow. If the proper distribution of boundary-layer displacement thickness is known, the local Y coordinates obtained by the equations of this report should be increased by this boundary-layer thickness. It is important to correct the shape of the straight-walled part of the nozzle for the boundary layer in order to avoid the emission of uncompensated compression waves that may produce a shock front somewhere in the flow.

FLIGHT PROPULSION RESEARCH LABORATORY,
NATIONAL ADVISORY COMMITTEE FOR AERONAUTICS,
CLEVELAND, OHIO, June 1, 1948.

APPENDIX A

SYMBOLS

The following symbols are used in this report and are illustrated in the figures:

A	area normal to flow direction (Because unit depth is assumed at all nozzle sections, the area at any section is numerically equal to the width of that section.)
A_1	source-flow area normal to flow direction at section where $M=1$ (equivalent throat area)
A_s	area normal to flow direction in expansive turn around corner
A_f	cross-sectional area of nozzle bearing uniform flow at M_f (nozzle exit)
A_r	source-flow area normal to flow lines at radial distance r from apparent source
A_t	nozzle-throat area
b, b_0, b_1, b_2	radial distances from "corner" to streamline representing adjacent nozzle wall (See figs. 11 to 14.)
D	displacement
d, d_0, d_1, d_2	radial distances from "corner" to streamline representing remote nozzle wall (See figs. 11 to 14.)
L	length of supersonic part of nozzle
L_s	length of initial expansion part
l	distance along characteristic from nozzle wall to limiting characteristic $(\Psi_-)_f$, $(\Psi_+)_E$, or $(\Psi_+)_S$
M	Mach number
M_E	Mach number of flow at circular-arc section E-E'
M_f	final Mach number of nozzle flow
M_l	Mach number of flow at section l-l'
M_n	Mach number of flow at first half of initial expansion part
M_r	Mach number of flow at circular-arc section bearing source flow at distance r from source
M_S	Mach number of flow at circular-arc section S-S'
r	radial distance along streamline or nozzle axis from apparent source
r_1	radial distance between apparent source and circular-arc section at which sonic velocity ($M=1$) exists in source flow
r_E	radial distance of circular-arc section E-E' from apparent source
r_f	radial distance between apparent source and location of point on axis where M_f is first attained
r_l	distance along nozzle axis from apparent source O to $(\Psi_+)_l$ or $(\Psi_-)_f$
r_S	radial distance of circular-arc section S-S' from apparent source
w_l	width of section l-l'
X, Y	nozzle-wall coordinates
X_1, Y_1	nozzle-wall coordinates of initial expansion part opposite first corner
X_2, Y_2	nozzle-wall coordinates of initial expansion part opposite second corner

X_f	distance of downstream end of nozzle from apparent source
X_l	distance of section l-l' from apparent source
x, y	coordinates of characteristic
α	inclination of nozzle wall to nozzle axis
α_E	maximum inclination of nozzle wall to nozzle axis (corresponds to wall inclination between circular-arc sections E-E' and S-S')
β	Mach angle ($\beta = \sin^{-1} 1/M$), angle between streamline and Mach line or characteristic
β_f	Mach angle in final uniform nozzle flow
β_l	Mach angle at section l-l'
β_n	Mach angle at first half of initial turning part
γ	ratio of specific heats
ζ	angle between characteristics bounding zone of expansion waves from corner C
θ	angle of inclination of streamline to nozzle axis
θ_{max}	one-half included angle between boundary streamlines of source flow (maximum possible θ in source flow)
λ	$= \sqrt{\frac{\gamma+1}{\gamma-1}}$
ξ	angle between downstream characteristic through corner C_2 and section l-l'
Ψ	equivalent Prandtl-Meyer turning angle
(Ψ_+)	characteristic originating at upper nozzle wall
(Ψ_-)	characteristic originating at lower nozzle wall
Ψ_f	value of Ψ at nozzle exit
Ψ_l	value of Ψ at section l-l'

Points along the nozzle wall or in the flow are designated by letters; letters for points along the lower nozzle wall are primed. Sections (cross sections through the two-dimensional flow, which are therefore only lines) are designated by the two letters ending the lines. Point-designation letters are in some places used as subscripts for clarity. Zones (region of different kinds of flow) are designated by Roman numerals; parts of the nozzle, which, like the zones, have two dimensions, are called by name. The following location letters are used:

C	corner in nozzle wall bounding sonic or supersonic flow
C'	corner in lower nozzle wall corresponding to C
E	point on upper nozzle wall at circular-arc section at which source flow is first established across entire channel of nozzle
E'	point on lower nozzle wall corresponding to E
l	point on upper nozzle wall representing downstream boundary of initial expansion part
l'	point on lower nozzle wall corresponding to l
O	apparent source
S	point on upper nozzle wall at last circular-arc section at which source flow exists across entire nozzle channel
S'	point on lower nozzle wall corresponding to S

Other capital letters are used to designate arbitrarily chosen points and as subscripts referring to those points; a, b, c , and d are used as subscripts in appendix B to indicate hypothetical values.

APPENDIX B

METHOD OF CHARACTERISTICS IN NOZZLE DESIGN

EXPANSION WAVES GENERATED AT CHANNEL WALLS

The form of the method of characteristics found most convenient for designing two-dimensional nozzles is described. Irrotational flows with total temperature and total pressure constant throughout the field are considered.

The starting point taken in setting up the method of characteristics used is conveniently discussed in terms of a uniform two-dimensional sonic or supersonic flow turning around a sharp corner of a wall along which the flow passes (fig. 18 (a)). The streamlines are turned about the corner with increasing Mach number, as at C_1 and C_2 , in wedge-shaped zones BC_1D and EC_2F , in which the static pressure decreases and the velocity increases in the direction of the flow. Such zones of decreasing pressure and increasing velocity are called expansion waves. Along radial lines through C_1 and C_2 the velocity, pressure, density, temperature, flow Mach number, and flow direction are constant. These radial lines are Mach lines that make the Mach angle

with the local flow direction $\beta = \sin^{-1} \frac{1}{M}$. Downstream of the bounding Mach line C_1D , the flow is uniform and parallel to wall C_1C_2 . At the corner in the wall at C_2 , the second wedge-shaped zone has a Mach line C_2E as the upstream boundary, which makes the same Mach angle β with the flow as does the Mach line C_1D because the flow between these two lines is uniform.

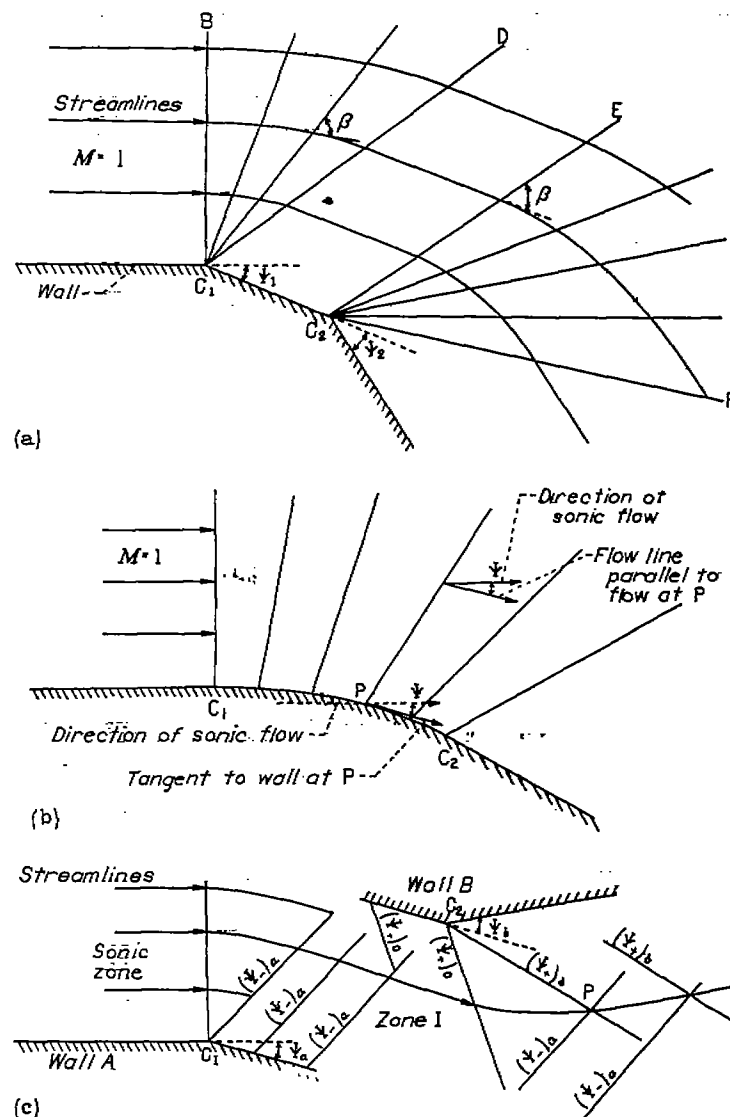
As the length of wall C_1C_2 has no effect on the direction and Mach number of the flow at line C_2E , the point C_2 could be made coincident with C_1 without altering the flow at C_2F . The change in Mach number and direction of the flow can therefore be considered to be a function only of the angle through which the flow is turned. Any stream tube having a supersonic Mach number can be considered to have come from a sonic flow ($M=1$) turned about a corner of angle Ψ . The expression relating the flow Mach number and corresponding turning angle (reference 2) is, in the notation of this paper,

$$\Psi = \lambda \tan^{-1} \frac{\sqrt{M^2 - 1}}{\lambda} - \tan^{-1} \sqrt{M^2 - 1} \quad (B1)$$

Because the Mach number of the flow is constant along Mach lines radiating from C_1 and C_2 , each Mach line is assigned a value of Ψ equal to the turning of the sonic flow required to give the corresponding Mach number. It is convenient to subscript these values of Ψ as $(\Psi)_n$ to indicate that the flow is deviated in a clockwise direction from the direction of the flow at sonic speed when crossing the Mach line originating at C_1 or C_2 . A Mach line to which a value of Ψ has been assigned will be called a characteristic. The angular turning of the flow produced by an expansion wave is equal to the difference in the values of Ψ of the characteristics bounding the wave. When the wall curves uniformly from C_1 to C_2 , as in figure 18 (b), at each point in the wall the turning of differential angle $d\Psi$ is considered to take place.

The wedge-shaped zone through each turn $d\Psi$ has a differential vertex angle at the wall and is simply represented by a single Mach line. The corresponding system of characteristics has the form shown in figure 18 (b). The flow across each characteristic is parallel to the flow at that point on the wall at which the characteristic originates.

If, after the turning of a sonic flow about a corner in wall A (fig. 18 (c)), a corner in wall B is encountered, the flow deviates in a counterclockwise direction around the corner in wall B. The change in Mach number of the flow due to the turn about wall B is the same as a similar turn around wall A with an initial Mach number equal to the value in zone I. If characteristics originating from wall B are



(a) Turning of sonic flow about two corners in wall.
 (b) Turning of sonic flow about smoothly curved wall.
 (c) Uniform supersonic flow about corners in two walls.

FIGURE 18.—Schematic representation of effect of tunnel-wall configuration on expansion waves and streamlines.

numbered according to the total counterclockwise angular deviation experienced by the flow arriving at the characteristics and indicated by (Ψ_+) , then the total turning experienced by the flow going from the sonic zone to point P (fig. 18 (c)), for example, is

$$\Psi = \Psi_a + \Psi_b = (\Psi_+)_b + (\Psi_-)_a = \lambda \tan^{-1} \frac{\sqrt{M^2 - 1}}{\lambda} - \tan^{-1} \sqrt{M^2 - 1} \quad (B2)$$

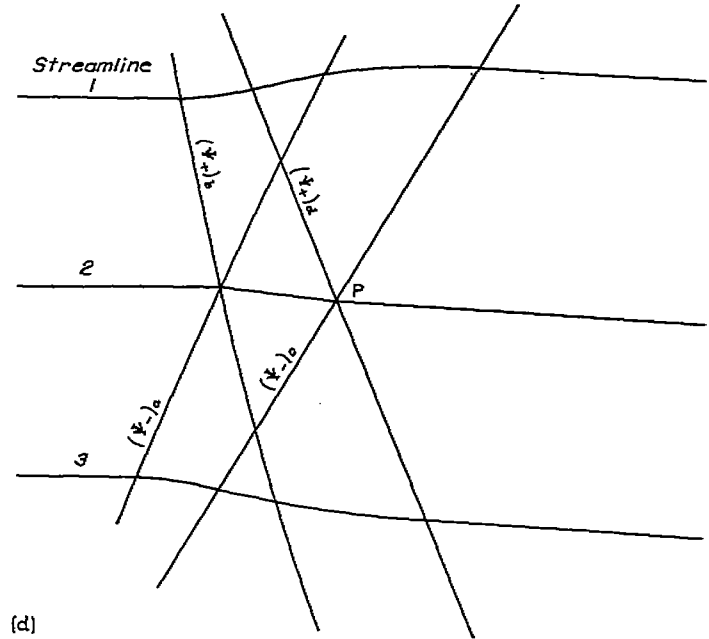
The net counterclockwise angular deviation of the flow along C_2P from the flow direction in the sonic zone is

$$\theta = (\Psi_+)_b - (\Psi_-)_a \quad (B3)$$

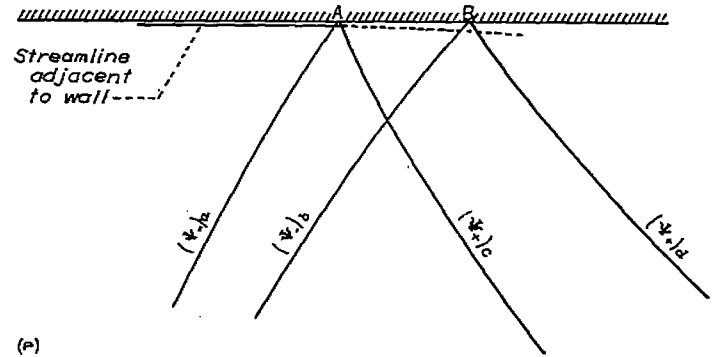
The values of the (Ψ_+) and (Ψ_-) characteristics downstream of point P are the same as at point P because no additional turning of the flow occurs downstream of C_2P .

Every point in a supersonic flow is crossed by two Mach lines making the Mach angle β with the flow direction. Because the characteristics are Mach lines numbered according to the convention just established, to every point in the supersonic flow a (Ψ_+) and a (Ψ_-) characteristic correspond. If the values of (Ψ_+) and (Ψ_-) are known at a point in the flow, the Mach number and the direction are given by equations (B2) and (B3).

The value of (Ψ_+) assigned to a characteristic is unaltered by its intersection with the characteristics of the (Ψ_-) set or vice versa. Two characteristics of the (Ψ_-) set are shown intersecting the two characteristics of the (Ψ_+) set in figure 18 (d). Three parallel streamlines, which may be considered to be elements of a supersonic stream tube are flowing across the characteristics. Streamline 1 is first given a counterclockwise deviation in flow path equal to $(\Psi_+)_a - (\Psi_+)_b$ in crossing the (Ψ_+) set of characteristics. It continues in a straight line until it intersects the set of (Ψ_-) characteristics, which give it a clockwise deviation in flow path equal to $(\Psi_-)_c - (\Psi_-)_a$. The net deflection in path in the counterclockwise direction is $[(\Psi_+)_a - (\Psi_+)_b] - [(\Psi_-)_c - (\Psi_-)_a]$. Streamline 3 intercepts the (Ψ_-) set of characteristics first and is deflected in a clockwise direction by an amount $(\Psi_-)_c - (\Psi_-)_a$. It continues in a straight line until it intercepts the (Ψ_+) set of characteristics, which deflect it in a counterclockwise direction an amount $(\Psi_+)_a - (\Psi_+)_b$. The net deflection of streamline 3 in the counterclockwise direction is $[(\Psi_+)_a - (\Psi_+)_b] - [(\Psi_-)_c - (\Psi_-)_a]$, the same as for streamline 1. The total turning $\Delta\Psi$ experienced by both streamlines 1 and 3 in crossing both sets of characteristics is the same and is equal to $[(\Psi_+)_a - (\Psi_+)_b] + [(\Psi_-)_c - (\Psi_-)_a]$. If streamlines 1 and 3 had the same Mach number and flow direction before intercepting the (Ψ_+) and (Ψ_-) set of characteristics, they would have the same new Mach number and new flow direction after crossing the characteristics. The stream-tube width has also increased to a value corresponding to the higher Mach number of flow after crossing the characteristics. Streamline 2 crosses both sets of characteristics simultaneously. Each set of charac-



(d)



(e)

(d) Flow through intersecting systems of characteristics.

(e) Expansion wave of Ψ_- set incident on straight wall.

FIGURE 18.—Continued. Schematic representation of effect of tunnel-wall configuration on expansion waves and streamlines.

teristics produces its turning of the flow independently of the other. The streamline assumes the resultant direction due to the simultaneous clockwise and counterclockwise turning of the flow. The final-flow direction and Mach number at P is the same as for streamlines 1 and 3 after passing through both sets of characteristics.

CHARACTERISTICS INCIDENT ON CHANNEL WALL

Only flows that do not separate from the confining channel walls are considered in this report. Consider two characteristics of the (Ψ_-) set, having values $(\Psi_-)_a$ and $(\Psi_-)_b$, incident on the straight channel wall shown in figure 18 (e). The streamlines move along the wall instead of following the dotted path under the influence of expansion waves contained between the (Ψ_-) characteristics because an expansion wave belonging to the (Ψ_+) set arises at the wall between points A and B that cancels the tendency of the flow to deviate from the wall. That is,

$$\Delta(\Psi_-) = (\Psi_-)_b - (\Psi_-)_a = \Delta(\Psi_+) = (\Psi_+)_a - (\Psi_+)_c \quad (B4)$$

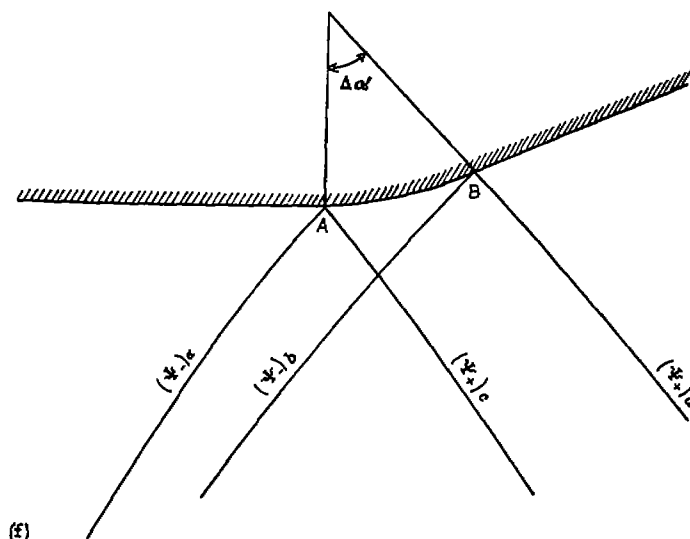
(f) Expansion wave of Ψ_- set incident on curved wall.

FIGURE 18.—Continued. Schematic representation of effect of tunnel-wall configuration on Mach waves and streamlines.

If, between points A and B, the wall curves (as in fig. 18 (f)) an amount $\Delta\alpha$, then the expansion wave of the (Ψ_+) set must exceed that of the incident (Ψ_-) set by an amount $\Delta\alpha$ or

$$\Delta(\Psi_+) = (\Psi_+)_a - (\Psi_+)_c = \Delta(\Psi_-) + \Delta\alpha = (\Psi_-)_b - (\Psi_-)_a + \Delta\alpha \quad (B5)$$

If between points A and B (fig. 18 (g)) the wall curves in the direction of the streamline along the wall under the

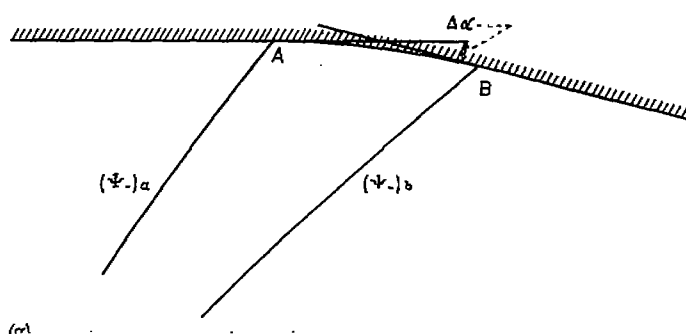
(g) Wall shape conforms to streamline curvature produced by incident expansion wave of Ψ_- set.

FIGURE 18.—Concluded. Schematic representation of effect of tunnel-wall configuration on expansion waves and streamlines.

influence of the wave of the (Ψ_-) set only, then the flow adjacent to the wall follows the wall without requiring the compensating expansion wave of the (Ψ_+) set. In this case no wave of the (Ψ_+) set is generated. The fact that waves emanating from a channel wall can be suppressed by curving the wall to the shape of the adjacent streamline under the influence of the incident expansion waves represents the basis of the method for designing supersonic nozzles used in this report.

The characteristics arising at a wall about which a two-dimensional flow is turned are straight as long as the flow responds to waves from only one wall. The deviation of the flow produced by an intersecting system of waves results in curved characteristics because the characteristics must make the Mach angle β everywhere with the flow direction.

APPENDIX C

DERIVATION OF EXPRESSION FOR MAXIMUM INITIAL EXPANSION ANGLE

In the discussion in appendix B of the expansive turning of a supersonic flow about a continuously curved wall (fig. 18 (b)), characteristics having a finite difference in turning angle were shown to have a finite distance of separation at the wall. If D be a displacement in the direction of the flow at the wall then

$$\frac{dD}{dM} > 0 \quad (C1)$$

In the limiting case of a sharp expansive turn (finite angle) at the wall, all characteristics in the corresponding wedge-shaped expansion wave originate at the sharp corner (fig. 18 (a)). The flow adjacent to the wall undergoes an abrupt finite increase in Mach number in crossing the wedge-shaped expansion wave at its vertex where the wave width dD in the direction of the flow is vanishingly small. In this case

$$\frac{dD}{dM} = 0 \quad (C2)$$

The condition expressed by equation (C2) represents a limiting value of $\frac{dD}{dM}$ because no expansive turn in a wall will give negative values for $\frac{dD}{dM}$ in the absence of waves incident upon the walls.

In the expansion part of the nozzles considered, no waves are incident upon the nozzle walls. Therefore the condition that $\frac{dD}{dM} \geq 0$ applies.

When a value of Ψ_I or M_I is chosen too low for the maximum wall-expansion angle α_E employed, then $\frac{dX}{dM}$ becomes negative in the neighborhood of section 1-1' where $\theta = 0$. For the limiting condition

$$\frac{dX}{dM} = 0 \quad (C3)$$

where X is the coordinate of the wall parallel to the nozzle axis (direction of flow at section 1-1' where $\alpha = 0$).

In order to obtain the allowable values of Ψ_I and α_E , as governed by equation (C3), the expression for X must be differentiated with respect to M and set equal to 0 at section 1-1', where $\theta = 0$, $M = M_I$, and $r = r_I$.

The expression for X for the expansion part of the nozzle is given by equation (13)

$$X = r \cos \theta - Mr(\alpha_E - \theta) \cos(\beta - \theta) \quad (C4)$$

and

$$\frac{dX}{dM} = \frac{\partial X}{\partial r} \frac{dr}{dM} + \frac{\partial X}{\partial \theta} \frac{d\theta}{dM} + \frac{\partial X}{\partial \beta} \frac{d\beta}{dM} + \frac{\partial X}{\partial M} = 0 \quad (C5)$$

From the values of the parameters at section 1-1', the terms in equation (C5) are obtained: From equation (1), with $\gamma = 1.40$,

$$r = \frac{r_I}{M} \left(\frac{5 + M^2}{6} \right)^3$$

$$\frac{dr}{dM} = r_I \left[\left(\frac{5 + M^2}{6} \right)^2 - \left(\frac{5 + M^2}{6} \right)^3 \frac{1}{M^2} \right] \quad (C6)$$

Substituting for r_I the expression preceding equation (C6) yields for section 1-1'

$$\frac{dr}{dM} = r_I \frac{5(M_I^2 - 1)}{M_I(5 + M_I^2)} \quad (C7)$$

and

$$\frac{\partial X}{\partial r} = \cos \theta - M(\alpha_E - \theta) \cos(\beta - \theta)$$

Because $\theta = 0$ and $M = M_I$,

$$\frac{\partial X}{\partial r} = 1 - M \alpha_E \cos \beta$$

$$\frac{\partial X}{\partial r} = 1 - \sqrt{M_I^2 - 1} \alpha_E \quad (C8)$$

From equation (11d), with $\gamma = 1.40$,

$$\theta = \Psi - \Psi_I = \lambda \tan^{-1} \frac{\sqrt{M^2 - 1}}{\lambda} - \tan^{-1} \sqrt{M^2 - 1} - \Psi_I$$

$$\begin{aligned} \frac{d\theta}{dM} &= \frac{M}{\left(1 + \frac{M^2 - 1}{\lambda^2}\right) \sqrt{M^2 - 1}} - \frac{1}{M \sqrt{M^2 - 1}} \\ &= \frac{5(M_I^2 - 1)}{M_I(5 + M_I^2) \sqrt{M_I^2 - 1}} \end{aligned} \quad (C9)$$

and

$$\frac{\partial X}{\partial \theta} = -r \sin \theta + Mr [\cos(\beta - \theta) - (\alpha_E - \theta) \sin(\beta - \theta)]$$

Therefore, for $\theta = 0$

$$\frac{\partial X}{\partial \theta} = r_I (\sqrt{M_I^2 - 1} - \alpha_E) \quad (C10)$$

By definition

$$\beta = \sin^{-1} \frac{1}{M} \quad (C11)$$

$$\frac{d\beta}{dM} = -\frac{1}{M_I \sqrt{M_I^2 - 1}}$$

From equation (C4)

$$\frac{\partial X}{\partial \beta} = Mr(\alpha_E - \theta) \sin(\beta - \theta)$$

which becomes at section $-l'$

$$\frac{\partial X}{\partial \beta} = r_I \alpha_E \quad (C12)$$

Also

$$\frac{\partial X}{\partial M} = -r(\alpha_E - \theta) \cos(\beta - \theta)$$

which gives, for $\theta = 0$

$$\frac{\partial X}{\partial M} = -\frac{\sqrt{M_I^2 - 1}}{M_I} r_I \alpha_E \quad (C13)$$

Substituting equations (C7) to (C13) in equation (C5) and solving for α_E yield equation (14):

$$\alpha_E = \frac{(M_I^2 - 1)^{3/2}}{0.6 M_I^4}$$

REFERENCES

1. Puckett, A. E.: Supersonic Nozzle Design. Jour. Appl. Mech., vol. 13, no. 4, Dec. 1946, pp. A265-A270.
2. Taylor, G. I., and Maccoll, J. W.: The Two-Dimensional Flow around a Corner; Two-Dimensional Flow past a Curved Surface. Vol. III of Aerodynamic Theory, div. H, ch. IV, secs. 5-6, W. F. Durand, ed., Julius Springer (Berlin), 1935, pp. 243-249.

TABLE I—VALUES OF β , Ψ , r/r_1 , AND d/d_0 FOR FIXED INTERVALS OF M

1	2	3	4	5	1	2	3	4	5	1	2	3	4	5
M, M_I	β (deg)	Ψ, Ψ_I $\Psi_I - \theta$ (deg)	$r \frac{2\alpha_E w_I}{A_I, d_0}$ $\frac{A_I}{A_I}, r$ $\frac{A_I}{A_I}, r_1$	$b \frac{d}{b_0, d_0}$	M, M_I	β (deg)	Ψ, Ψ_I $\Psi_I - \theta$ (deg)	$r \frac{2\alpha_E w_I}{A_I, d_0}$ $\frac{A_I}{A_I}, r$ $\frac{A_I}{A_I}, r_1$	$b \frac{d}{b_0, d_0}$	M, M_I	β (deg)	Ψ, Ψ_I $\Psi_I - \theta$ (deg)	$r \frac{2\alpha_E w_I}{A_I, d_0}$ $\frac{A_I}{A_I}, r$ $\frac{A_I}{A_I}, r_1$	$b \frac{d}{b_0, d_0}$
1.00	90.000	0.000	1.0000	1.0000	2.00	30.000	26.380	1.6875	3.3750	3.00	19.471	49.767	4.2340	12.7037
1.02	78.636	.128	1.0303	1.0203	2.02	29.673	26.929	1.7160	3.4063	3.02	19.337	50.142	4.3160	13.0343
1.04	74.058	.351	1.0613	1.0414	2.04	29.353	27.476	1.7451	3.5001	3.04	19.206	50.523	4.3989	13.3728
1.06	70.630	.637	1.0929	1.0631	2.06	29.041	28.022	1.7750	3.5856	3.06	19.074	50.902	4.4835	13.7104
1.08	67.808	.968	1.0051	1.0955	2.08	28.736	28.562	1.8056	3.7587	3.08	18.946	51.277	4.5696	14.0743
1.10	65.280	1.336	1.0079	1.1087	2.10	28.437	29.097	1.8360	3.8576	3.10	18.819	51.650	4.6573	14.4377
1.12	63.234	1.735	1.0113	1.1327	2.12	28.145	29.631	1.8680	3.9623	3.12	18.694	52.020	4.7467	14.8096
1.14	61.306	2.160	1.0153	1.1574	2.14	27.859	30.161	1.9018	4.0999	3.14	18.570	52.386	4.8377	15.1903
1.16	59.530	2.607	1.0198	1.1829	2.16	27.578	30.688	1.9354	4.1805	3.16	18.449	52.750	4.9304	15.5800
1.18	57.936	3.074	1.0248	1.2093	2.18	27.304	31.213	1.9698	4.2942	3.18	18.328	53.112	5.0245	15.9789
1.20	56.443	3.558	1.0304	1.2365	2.20	27.036	31.732	2.0050	4.4109	3.20	18.210	53.470	5.1210	16.3871
1.22	55.052	4.057	1.0366	1.2646	2.22	26.773	32.250	2.0409	4.5309	3.22	18.093	53.826	5.2189	16.8048
1.24	53.761	4.570	1.0432	1.2936	2.24	26.515	32.768	2.0777	4.6541	3.24	17.977	54.179	5.3186	17.2321
1.26	52.528	5.093	1.0501	1.3235	2.26	26.262	33.274	2.1154	4.7807	3.26	17.863	54.530	5.4201	17.6694
1.28	51.375	5.627	1.0581	1.3544	2.28	26.014	33.778	2.1538	4.9107	3.28	17.751	54.877	5.5234	18.1168
1.30	50.285	6.170	1.0668	1.3862	2.30	25.772	34.283	2.1931	5.0442	3.30	17.640	55.222	5.6286	18.5745
1.32	49.251	6.721	1.0750	1.4190	2.32	25.533	34.783	2.2333	5.1813	3.32	17.530	55.564	5.7358	19.0427
1.34	48.268	7.279	1.0842	1.4529	2.34	25.300	35.279	2.2744	5.3221	3.34	17.422	55.904	5.8445	19.5216
1.36	47.332	7.844	1.0940	1.4878	2.36	25.070	35.771	2.3164	5.4666	3.36	17.316	56.241	5.9558	20.0114
1.38	46.439	8.413	1.1042	1.5233	2.38	24.845	36.262	2.3593	5.6151	3.38	17.209	56.576	6.0687	20.5123
1.40	45.585	8.987	1.1149	1.5603	2.40	24.624	36.746	2.4031	5.7674	3.40	17.105	56.908	6.1837	21.0245
1.42	44.767	9.566	1.1262	1.5982	2.42	24.407	37.230	2.4479	5.9238	3.42	17.003	57.238	6.3007	21.5484
1.44	43.988	10.146	1.1379	1.6366	2.44	24.195	37.708	2.4936	6.0844	3.44	16.900	57.564	6.4198	22.0840
1.46	43.230	10.730	1.1502	1.6752	2.46	23.986	38.184	2.5403	6.2492	3.46	16.799	57.888	6.5409	22.6316
1.48	42.507	11.327	1.1631	1.7141	2.48	23.780	38.655	2.5880	6.4188	3.48	16.700	58.210	6.6642	23.1914
1.50	41.810	11.936	1.1762	1.7532	2.50	23.578	39.124	2.6367	6.5918	3.50	16.602	58.530	6.7896	23.7637
1.52	41.140	12.498	1.1899	1.7927	2.52	23.380	39.589	2.6864	6.7688	3.52	16.504	58.847	6.9172	24.3486
1.54	40.493	13.085	1.2042	1.8325	2.54	23.185	40.050	2.7372	6.9526	3.54	16.409	59.162	7.0470	24.9460
1.56	39.868	13.675	1.2190	1.8726	2.56	22.993	40.508	2.7891	7.1400	3.56	16.314	59.474	7.1791	25.5577
1.58	39.265	14.270	1.2344	1.9130	2.58	22.805	40.963	2.8420	7.3323	3.58	16.220	59.784	7.3135	26.1822
1.60	38.682	14.880	1.2502	1.9538	2.60	22.620	41.415	2.8960	7.5295	3.60	16.128	60.091	7.4501	26.8204
1.62	38.118	15.492	1.2666	1.9950	2.62	22.438	41.863	2.9511	7.7318	3.62	16.036	60.397	7.5881	27.4725
1.64	37.572	16.043	1.2835	2.0365	2.64	22.259	42.308	3.0073	7.9394	3.64	15.946	60.700	7.7304	28.1386
1.66	37.043	16.633	1.3010	2.0782	2.66	22.082	42.749	3.0647	8.1522	3.66	15.850	61.000	7.8742	28.8190
1.68	36.530	17.223	1.3190	2.1200	2.68	21.909	43.187	3.1233	8.3704	3.68	15.758	61.299	8.0204	29.5161
1.70	36.032	17.810	1.3376	2.1629	2.70	21.738	43.621	3.1830	8.5941	3.70	15.660	61.595	8.1690	30.2255
1.72	35.549	18.397	1.3567	2.2068	2.72	21.571	44.053	3.2440	8.8235	3.72	15.564	61.889	8.3203	30.9512
1.74	35.080	18.981	1.3764	2.2510	2.74	21.405	44.481	3.3061	9.0587	3.74	15.468	62.181	8.4739	31.6925
1.76	34.624	19.566	1.3967	2.2962	2.76	21.243	44.906	3.3695	9.2998	3.76	15.374	62.471	8.6302	32.4495
1.78	34.180	20.146	1.4175	2.3422	2.78	21.082	45.328	3.4342	9.5470	3.78	15.280	62.763	8.7891	33.2227
1.80	33.749	20.726	1.4390	2.3892	2.80	20.925	45.746	3.5001	9.8003	3.80	15.188	63.044	8.9506	34.0122
1.82	33.329	21.304	1.4610	2.4369	2.82	20.770	46.161	3.5674	10.0600	3.82	15.096	63.327	9.1148	34.8184
1.84	32.921	21.878	1.4836	2.4852	2.84	20.617	46.573	3.6359	10.3260	3.84	15.005	63.608	9.2817	35.6416
1.86	32.523	22.450	1.5069	2.5342	2.86	20.466	46.982	3.7058	10.5987	3.86	14.915	63.887	9.4513	36.4820
1.88	32.135	23.020	1.5307	2.5838	2.88	20.318	47.388	3.7771	10.8781	3.88	14.826	64.164	9.6237	37.3401
1.90	31.757	23.586	1.5553	2.6340	2.90	20.171	47.790	3.8498	11.1643	3.90	14.737	64.440	9.7990	38.2160
1.92	31.388	24.152	1.5804	2.6848	2.92	20.027	48.190	3.9235	11.4576	3.92	14.648	64.713	9.9771	39.1101
1.94	31.028	24.713	1.6062	2.7362	2.94	19.885	48.586	3.9983	11.7589	3.94	14.559	64.984	10.1580	40.0227
1.96	30.677	25.270	1.6326	2.7882	2.96	19.745	48.980	4.0763	12.0657	3.96	14.472	65.253	10.3420	40.9542
1.98	30.335	25.827	1.6597	2.8408	2.98	19.607	49.370	4.1547	12.3809	3.98	14.385	65.520	10.5288	41.9019

TABLE I—VALUES OF β , Ψ , r/r_1 , AND d/d_0 FOR FIXED INTERVALS OF M —Concluded

1	2	3	4	5	1	2	3	4	5	1	2	3	4	5
$M, M_f,$ M_t	β (deg)	$\Psi, \Psi_f,$ $\Psi_f - \theta$ (deg)	$r \frac{2\alpha_B w_f}{A_t d_0},$ $\frac{A_f}{A_t} \frac{r}{r_1}$	$b \frac{d}{b_0 d_0}$	$M, M_f,$ M_t	β (deg)	$\Psi, \Psi_f,$ $\Psi_f - \theta$ (deg)	$r \frac{2\alpha_B w_f}{A_t d_0},$ $\frac{A_f}{A_t} \frac{r}{r_1}$	$b \frac{d}{b_0 d_0}$	$M, M_f,$ M_t	β (deg)	$\Psi, \Psi_f,$ $\Psi_f - \theta$ (deg)	$r \frac{2\alpha_B w_f}{A_t d_0},$ $\frac{A_f}{A_t} \frac{r}{r_1}$	$b \frac{d}{b_0 d_0}$
4.00	14.478	65.785	10.719	42.875	6.00	9.594	84.955	53.178	319.07	8.00	7.181	95.627	190.109	1520.88
4.05	14.295	66.439	11.207	45.353	6.05	9.514	85.299	55.101	333.36	8.05	7.136	95.832	195.597	1574.56
4.10	14.117	67.085	11.715	48.030	6.10	9.435	85.634	57.077	348.17	8.10	7.092	96.033	201.215	1629.84
4.15	13.943	67.714	12.243	50.809	6.15	9.358	85.968	59.114	363.55	8.15	7.048	96.234	206.964	1686.76
4.20	13.774	68.334	12.791	53.724	6.20	9.282	86.296	61.210	379.50	8.20	7.005	96.431	212.846	1745.34
4.25	13.609	68.945	13.363	56.792	6.25	9.207	86.618	63.370	396.06	8.25	6.962	96.625	218.865	1805.64
4.30	13.448	69.541	13.955	60.006	6.30	9.133	86.938	65.589	413.21	8.30	6.920	96.821	225.022	1867.68
4.35	13.290	70.128	14.571	63.383	6.35	9.061	87.251	67.877	431.02	8.35	6.878	97.013	231.320	1931.53
4.40	13.137	70.707	15.210	66.923	6.40	8.989	87.561	70.226	449.46	8.40	6.837	97.199	237.763	1997.21
4.45	12.986	71.274	15.874	70.638	6.45	8.919	87.868	72.647	468.57	8.45	6.796	97.388	244.350	2064.76
4.50	12.840	71.833	16.562	74.529	6.50	8.850	88.169	75.134	488.37	8.50	6.756	97.573	251.086	2134.23
4.55	12.696	72.380	17.277	78.612	6.55	8.782	88.466	77.695	508.90	8.55	6.717	97.767	257.974	2205.68
4.60	12.556	72.919	18.018	82.882	6.60	8.715	88.759	80.323	530.13	8.60	6.677	97.958	265.014	2279.12
4.65	12.419	73.448	18.787	87.358	6.65	8.649	89.051	83.027	552.13	8.65	6.639	98.118	272.211	2354.63
4.70	12.284	73.969	19.583	92.039	6.70	8.584	89.336	85.804	574.89	8.70	6.600	98.294	279.587	2432.24
4.75	12.153	74.483	20.409	96.943	6.75	8.520	89.618	88.681	598.46	8.75	6.562	98.469	287.084	2511.99
4.80	12.026	74.996	21.263	102.06	6.80	8.457	89.895	91.594	622.84	8.80	6.525	98.643	294.766	2593.94
4.85	11.899	75.483	22.151	107.43	6.85	8.394	90.170	94.609	647.13	8.85	6.488	98.814	302.615	2678.14
4.90	11.776	75.970	23.077	113.03	6.90	8.333	90.442	97.700	672.42	8.90	6.451	98.983	310.633	2764.63
4.95	11.655	76.451	24.018	118.89	6.95	8.273	90.710	100.880	701.11	8.95	6.415	99.153	318.823	2853.47
5.00	11.537	76.921	25.000	125.00	7.00	8.213	90.974	104.143	729.00	9.00	6.379	99.320	327.190	2944.71
5.05	11.421	77.383	26.018	131.39	7.05	8.155	91.237	107.492	757.82	9.05	6.344	99.483	335.733	3038.39
5.10	11.308	77.841	27.069	138.05	7.10	8.097	91.492	110.931	787.61	9.10	6.309	99.647	344.458	3134.57
5.15	11.197	78.293	28.169	145.02	7.15	8.040	91.746	114.459	818.36	9.15	6.274	99.808	353.368	3233.32
5.20	11.088	78.735	29.283	152.27	7.20	7.984	91.999	118.080	850.18	9.20	6.240	99.967	362.463	3334.66
5.25	10.981	79.170	30.446	159.84	7.25	7.928	92.244	121.794	883.01	9.25	6.206	100.127	371.749	3438.68
5.30	10.876	79.599	31.649	167.74	7.30	7.873	92.491	125.605	916.91	9.30	6.178	100.282	381.228	3545.42
5.35	10.773	80.017	32.893	175.98	7.35	7.820	92.731	129.513	951.92	9.35	6.140	100.438	390.902	3654.93
5.40	10.672	80.433	34.174	184.54	7.40	7.766	92.971	133.520	988.05	9.40	6.107	100.591	400.775	3767.29
5.45	10.573	80.844	35.501	193.45	7.45	7.714	93.206	137.629	1025.34	9.45	6.074	100.742	410.851	3882.54
5.50	10.476	81.244	36.869	202.78	7.50	7.662	93.441	141.842	1063.81	9.50	6.042	100.891	421.131	4000.75
5.55	10.380	81.643	38.281	212.46	7.55	7.611	93.671	146.169	1103.64	9.55	6.011	101.041	431.620	4121.97
5.60	10.287	82.032	39.741	222.55	7.60	7.561	93.898	150.685	1144.45	9.60	5.979	101.188	442.322	4246.29
5.65	10.195	82.418	41.246	233.04	7.65	7.511	94.122	155.120	1186.87	9.65	5.948	101.334	453.236	4373.73
5.70	10.104	82.795	42.796	243.94	7.70	7.462	94.345	159.707	1230.23	9.70	5.917	101.478	464.370	4504.39
5.75	10.015	83.171	44.400	255.30	7.75	7.414	94.567	164.627	1275.08	9.75	5.887	101.623	475.725	4638.32
5.80	9.928	83.537	46.050	267.09	7.80	7.366	94.783	169.403	1321.35	9.80	5.857	101.764	487.304	4775.58
5.85	9.842	83.900	47.754	279.38	7.85	7.319	94.988	174.418	1369.02	9.85	5.827	101.903	499.112	4916.25
5.90	9.758	84.257	49.507	292.09	7.90	7.272	95.199	179.511	1418.14	9.90	5.797	102.042	511.132	5060.40
5.95	9.675	84.607	51.315	305.34	7.95	7.226	95.417	184.744	1468.72	9.95	5.768	102.180	523.425	5208.08
										10.00	5.739	102.317	536.938	5359.38

TABLE II—VALUES OF M , β , r/r_1 , d/d_0 , FOR FIXED INTERVALS OF Ψ

[Values obtained by interpolation from table I]

1	2	3	4	5	1	2	3	4	5	1	2	3	4	5
$\Psi, \Psi_f,$ $\Psi_f - \theta$ (deg)	M, M_f	β (deg)	$r \frac{2\alpha_E w_f}{A_t}, \frac{w_f}{d_0},$ $\frac{A_f}{A_t}, \frac{r}{r_1}$	$\frac{b}{b_0}, \frac{d}{d_0}$	$\Psi, \Psi_f,$ $\Psi_f - \theta$ (deg)	M, M_f	β (deg)	$r \frac{2\alpha_E w_f}{A_t}, \frac{w_f}{d_0},$ $\frac{A_f}{A_t}, \frac{r}{r_1}$	$\frac{b}{b_0}, \frac{d}{d_0}$	$\Psi, \Psi_f,$ $\Psi_f - \theta$ (deg)	M, M_f	β (deg)	$r \frac{2\alpha_E w_f}{A_t}, \frac{w_f}{d_0},$ $\frac{A_f}{A_t}, \frac{r}{r_1}$	$\frac{b}{b_0}, \frac{d}{d_0}$
0	1.0000	90.000	1.0000	1.0000	13.5	1.5541	40.053	1.2146	1.8877	27.0	2.0226	29.631	1.7198	3.4783
.5	1.0504	72.272	1.0021	1.0527	14.0	1.5709	39.539	1.2274	1.9282	27.5	2.0409	29.339	1.7464	3.5043
1.0	1.0817	67.597	1.0053	1.0875	14.5	1.5878	39.038	1.2406	1.9698	28.0	2.0592	29.058	1.7738	3.5306
1.5	1.1082	64.498	1.0098	1.1186	15.0	1.6047	38.549	1.2541	2.0126	28.5	2.0777	28.771	1.8021	3.5574
2.0	1.1325	62.032	1.0138	1.1481	15.5	1.6216	38.074	1.2680	2.0582	29.0	2.0964	28.491	1.8312	3.5891
2.5	1.1552	59.970	1.0187	1.1768	16.0	1.6385	37.612	1.2823	2.1011	29.5	2.1151	28.217	1.8611	3.6366
3.0	1.1768	58.192	1.0240	1.2051	16.5	1.6555	37.162	1.2971	2.1474	30.0	2.1339	27.948	1.8918	3.6872
3.5	1.1976	56.622	1.0297	1.2332	17.0	1.6724	36.724	1.3122	2.1947	30.5	2.1529	27.678	1.9234	3.7410
4.0	1.2177	55.211	1.0359	1.2614	17.5	1.6894	36.295	1.3278	2.2433	31.0	2.1719	27.410	1.9569	3.7981
4.5	1.2373	53.929	1.0423	1.2896	18.0	1.7065	35.876	1.3438	2.2932	31.5	2.1911	27.146	1.9923	3.8586
5.0	1.2564	52.745	1.0491	1.3182	18.5	1.7236	35.466	1.3602	2.3444	32.0	2.2103	26.880	2.0293	3.9226
5.5	1.2752	51.649	1.0563	1.3471	19.0	1.7407	35.065	1.3771	2.3971	32.5	2.2297	26.617	2.0678	3.9901
6.0	1.2937	50.626	1.0637	1.3762	19.5	1.7577	34.675	1.3944	2.4511	33.0	2.2493	26.359	2.1078	4.0611
6.5	1.3120	49.666	1.0715	1.4058	20.0	1.7750	34.292	1.4123	2.5063	33.5	2.2690	26.101	2.1493	4.1356
7.0	1.3300	48.759	1.0796	1.4360	20.5	1.7922	33.917	1.4306	2.5642	34.0	2.2888	25.848	2.1923	4.2136
7.5	1.3478	47.902	1.0880	1.4666	21.0	1.8095	33.549	1.4495	2.6229	34.5	2.3087	25.598	2.2368	4.2951
8.0	1.3655	47.087	1.0968	1.4977	21.5	1.8268	33.190	1.4687	2.6832	35.0	2.3288	25.351	2.2828	4.3801
8.5	1.3830	46.310	1.1058	1.5294	22.0	1.8443	32.838	1.4882	2.7454	35.5	2.3490	25.107	2.3303	4.4686
9.0	1.4005	45.567	1.1152	1.5618	22.5	1.8618	32.499	1.5080	2.8094	36.0	2.3693	24.866	2.3793	4.5606
9.5	1.4178	44.869	1.1249	1.5949	23.0	1.8793	32.149	1.5289	2.8762	36.5	2.3898	24.628	2.4298	4.6561
10.0	1.4350	44.180	1.1350	1.6287	23.5	1.8970	31.814	1.5516	2.9433	37.0	2.4105	24.393	2.4818	4.7551
10.5	1.4521	43.527	1.1454	1.6632	24.0	1.9146	31.487	1.5757	3.0130	37.5	2.4313	24.161	2.5353	4.8576
11.0	1.4690	42.903	1.1569	1.6982	24.5	1.9324	31.165	1.5964	3.0850	38.0	2.4523	23.932	2.5903	4.9636
11.5	1.4860	42.299	1.1689	1.7340	25.0	1.9503	30.847	1.6198	3.1592	38.5	2.4734	23.707	2.6468	5.0736
12.0	1.5032	41.703	1.1784	1.7713	25.5	1.9683	30.536	1.6438	3.2356	39.0	2.4947	23.483	2.7048	5.1876
12.5	1.5202	41.124	1.1900	1.8091	26.0	1.9868	30.230	1.6684	3.3140	39.5	2.5162	23.261	2.7643	5.3056
13.0	1.5371	40.566	1.2021	1.8479	26.5	2.0044	29.929	1.6937	3.3950	40.0	2.5378	23.036	2.8253	5.4276

TABLE III—SAMPLE DESIGN OF TWO-DIMENSIONAL SUPERSONIC NOZZLES FOR FINAL MACH NUMBER M_f OF 3.50 AND FINAL NOZZLE WIDTH OF 10 INCHES

[Symbols defined in appendix A]

(a) Design parameters

Equation	Equation number	Shortest nozzle ¹				Nozzle with straight-walled part ²			
		Source of computed value			Value	Source of computed value			Value
		Table	Figure	Computation		Table	Figure	Computation	
$\frac{A_f}{A_t} = \frac{1}{M} \left(\frac{1 + \frac{\gamma-1}{2} M^2}{\frac{\gamma+1}{2}} \right)^{\frac{\gamma+1}{2(\gamma-1)}}$		I, col. 4, $M_f=3.50$			6.7896	I, col. 4, $M_f=3.50$			6.7896
$A_t = \left(\frac{A_f}{A_t} \right) A_f$				$\frac{1}{6.7896} \times 10$	1.4728 in.			$\frac{1}{6.7896} \times 10$	1.4728 in.
$d_0 = A_t$ (numerically)					1.4728 in.				1.4728 in.
Ψ_f		I, col. 3, $M_f=3.50$			58.530°	I, col. 3, $M_f=3.50$			58.530°
Ψ_f			6(b) $M=3.50$	(For convenience)	9.8° 10.000°			α_B given (15.000°) $M_f=1.222$ (fig. 8)	4.108°, or 5.000° for convenience
$\alpha_B = \frac{\Psi_f - \Psi_t}{2}$	19c			$\frac{58.530^\circ - 10.000^\circ}{2}$	24.265° or 0.4235 rad.	I, Ψ_t , $M_t=1.222$	8, M_t		15.000° given
M_t		II, col. 2, $\Psi_t=10.0^\circ$			1.4350	II, col. 2, $\Psi_t=5.000^\circ$			1.2504
β_t		II, col. 3, $\Psi_t=10.0^\circ$			44.180°	II, col. 3, $\Psi_t=5.000^\circ$			52.745°
$\Psi_B = \Psi_t + \alpha_B$	20a			10.000° + 24.265°	34.265°			5.000° + 15.000°	20.000°
M_B		II, col. 2, $\Psi_B=34.265^\circ$			2.2693	II, col. 2, $\Psi_B=20.000^\circ$			1.7750
Ψ_B	20b							58.530° - 15.000°	43.530°
M_B						I, col. 3, $\Psi_B=43.530^\circ$			2.6958
r_t	14b			$\frac{1.4728}{2 \times 0.42350}$	1.7388			$\frac{1.4728}{2 \times 0.26180}$	2.8128

(b) Typical coordinates of expansion part ($M=1.600$)

Equation	Equation number	Shortest nozzle ¹			Nozzle with straight-walled part ²		
		Source of computed value		Value	Source of computed value		Value
		Table	Computation		Table	Computation	
M	$M_t \leq M \leq M_B$		$1.4350 \leq M \leq 2.2693$ (Value chosen)	1.600		$1.222 \leq M \leq 1.775$ (Value chosen)	1.600
Ψ		I, col. 3, $M=1.60$		14.860°	I, col. 3, $M=1.60$		14.860°
θ	$\Psi - \Psi_t$	11d	14.860° - 10.000°	4.860°		14.860° - 5.000°	9.860°
$\frac{r}{r_t}$		11b	I, col. 4, $M=1.60$	1.2502	I, col. 4, $M=1.60$		1.2502
r	$\frac{r}{r_t} r_t$		1.2502×1.7388	2.1738 in.		1.2502×2.8128	3.5166 in.
β	$\sin^{-1} \frac{1}{M}$	I, col. 2, $M=1.60$		38.682°	I, col. 2, $M=1.60$		38.682°
$\alpha_B - \theta$			24.265° - 4.860°	19.405° .33868 rad.		15.000° - 9.860°	5.14° .08971 rad.
$\beta - \theta$			38.682° - 4.860°	33.822°		38.682° - 9.860°	28.822°
X	$r \cos \theta - M r (\alpha_B - \theta) \cos (\beta - \theta)$	13	$2.1738 \cos 4.860 - 1.6 \times 2.1738 \times .33868 \cos 33.822$	1.187 in.		$3.5166 \cos 9.860 - 1.6 \times 3.5166 \times .08971 \cos 28.822$	3.022 in.
Y	$r \sin \theta + M r (\alpha_B - \theta) \sin (\beta - \theta)$	13a	$2.1738 \sin 4.860 + 1.6 \times 2.1738 \times .33868 \sin 33.822$	0.840 in.		$3.5166 \sin 9.860 + 1.6 \times 3.5166 \times .08971 \sin 28.822$	0.810 in.

(c) Length of straight-walled part (equation (20))

$\frac{r_B}{A_t} = \frac{r_B}{2\alpha_B}$	$\frac{r_B}{r_t}$				I, col. 4, $M_B=2.6958$		3.1705
$\frac{r_B}{A_t} = \frac{r_B}{2\alpha_B}$	$\frac{r_B}{r_t}$				I, col. 4, $M_B=1.775$		1.4123
$r_B - r_t$	$\left(\frac{r_B}{A_t} - \frac{r_t}{A_t} \right) \frac{A_t}{2\alpha_B}$					$(3.1705 - 1.4123) \times 2.8128$	4.9455 in.

¹ No straight-walled part; initial expansion accomplished by 1 turn about sharp corner.² Straight-walled part with α_B of 15.000°; initial expansion accomplished by 2 turns in succession about sharp corner at each wall.

TABLE III—SAMPLE DESIGN OF TWO-DIMENSIONAL SUPERSONIC NOZZLES FOR FINAL MACH NUMBER M_f OF 3.50 AND FINAL NOZZLE WIDTH OF 10 INCHES—Continued(d) Typical coordinate of straightening part ($M=2.80$)

Equation	Equation number	Shortest nozzle ¹			Nozzle with straight-walled part ²		
		Source of computed value		Value	Source of computed value		Value
		Table	Computation		Table	Computation	
M	$M_s \leq M \leq M_f$		$M_s = M_s 2.2993 \leq M \leq 3.50$ (Value chosen)	2.800		$2.6958 \leq M \leq 3.50$ (Value chosen)	2.800
Ψ		I, col. 3, $M=2.80$		45.746°	I, col. 3, $M=2.80$		45.746°
θ	$\Psi_f - \Psi$	16a		58.530° - 45.746°		58.530° - 45.746°	12.784°
$\frac{r}{r_1}$		I, col. 4, $M=2.80$		3.5001	I, col. 4, $M=2.80$		3.5001
r	$\left(\frac{r}{r_1}\right) r_1$			3.5001 × 1.7368		3.5001 × 2.8128	9.8451 in.
β		I, col. 2, $M=2.80$		20.925	I, col. 2, $M=2.80$		20.925
$\alpha_s - \theta$				24.265° - 12.784°		15.000° - 12.784°	2.216°
				0.2003 rad.			0.0387 rad.
$\beta + \theta$				20.925° + 12.784°		20.925° + 12.784°	33.709°
X	$r \cos \theta + Mr (\alpha_s - \theta) \cos (\beta + \theta)$	18		6.0860 cos 12.784° + 2.8 × 6.0860 × 0.2003 cos 33.709°		9.8451 cos 12.784° + 2.8 × 9.8451 × 0.0387 cos 33.709°	10.489 in.
Y	$r \sin \theta + Mr (\alpha_s - \theta) \sin (\beta + \theta)$	18a		6.0860 sin 12.784° + 2.8 × 6.0860 × 0.2003 sin 33.709°		9.8451 sin 12.784° + 2.8 × 9.8451 × 0.0387 sin 33.709°	2.771 in.

(e) Typical coordinates of initial expansion part

Equation	Equation number	Shortest nozzle with single initial turn; $\Psi_I=10.000^\circ$ ¹				Nozzle with straight-walled part and double initial turn; $\Psi_I=5.000^\circ$ ²			
		Source of computed value		Value	Source of computed value		Value		
		Table	Computation		Table	Computation			
First turn									
$\frac{\Psi_I}{2}$						$\frac{5.000}{2}$		2.500°	
M_s					II, col. 2, $\Psi_s=2.5^\circ$			1.1552	
M	$1 \leq M \leq M_I, 1 \leq M \leq M_s$		$1 \leq M \leq 1.4350$ (Value chosen)	1.2400		$1 \leq M \leq 1.1552$ (Value chosen)		1.1400	
β		I, col. 2, $M=1.24$		53.751°	I, col. 2, $M=1.14$			61.306°	
Ψ		I, col. 3, $M=1.24$		4.570°	I, col. 3, $M=1.14$			2.160°	
$\beta+\Psi_I-\Psi$			$53.751+10.000-4.570$	59.181°					
$\beta+\frac{\Psi_I}{2}-\Psi$						$61.306+2.500-2.160$		61.646°	
$\frac{d_1}{d_0}$		I, col. 5, $M=1.24$		1.2936	I, col. 5, $M=1.14$			1.1574	
d_1	$\frac{d_1}{d_0} d_0$		1.2936×1.4728	1.9052 in.		1.1574×1.4728		1.7046 in.	
X_1	$d_1 \cos (\beta+\Psi_I-\Psi)$	28a	$1.9052 \cos 59.181$	0.976 in.		$1.7046 \cos 61.646$		0.810 in.	
Y_1	$d_1 \sin (\beta+\Psi_I-\Psi)$	28b	$1.9052 \sin 59.181$	1.536 in.		$1.7046 \sin 61.646$		1.500 in.	
Second turn									
M	$M_s \leq M \leq M_I$					$1.1552 \leq M \leq 1.2564$ (Value chosen)		1.2200	
β					I, col. 2, $M=1.22$			55.052°	
Ψ					I, col. 3, $M=1.22$			4.057°	
$\beta+\Psi_I-\Psi$						$55.052+5.000-4.057$		55.995°	
$\frac{d_2}{d_0}$					I, col. 5, $M=1.22$			1.2646	
d_2	$(d_2/d_0) d_0$					1.2646×1.4728		1.8625 in.	
X_2	$d_2 \cos (\beta+\Psi_I-\Psi)$	30a				$1.8625 \cos 55.995$		1.042 in.	
Y_2	$d_2 \sin (\beta+\Psi_I-\Psi)$					$1.8625 \sin 55.995$		1.544 in.	

¹ No straight-walled part; initial expansion accomplished by 1 turn about sharp corner.² Straight-walled part with α_s of 15.000°; initial expansion accomplished by 2 turns in succession about sharp corner at each wall.

TABLE III—SAMPLE DESIGN OF TWO-DIMENSIONAL SUPERSONIC NOZZLES FOR FINAL MACH NUMBER M_f OF 3.50 AND FINAL NOZZLE WIDTH OF 10 INCHES—Concluded

(f) Nozzle length

Equation	Equation number	Shortest nozzle ¹			Nozzle with straight-walled part ²			
		Source of computed value		Value	Source of computed value		Value	
		Table	Computation		Table	Computation		
Expansion, straight-walled, and straightening part								
			I, col. 2, $M_f=3.50$	16.602°	I, col. 2, $M_f=3.50$		16.602°	
$\frac{r_f}{r_i}$			I, col. 4, $M_f=3.50$	6.7896	I, col. 4, $M_f=3.50$		6.7896	
r_f	$\frac{r_f}{r_i} r_i$			6.7896×1.7388	11.806 in.		6.7896×2.8128	19.098 in.
$\frac{r_f}{r_i}$			II, col. 4, $\Psi_f=10.000^\circ$		1.1350	II, col. 4, $\Psi_f=5.000^\circ$		1.0491
r_f	$\frac{r_f}{r_i} r_i$			1.1350×1.7388	1.9735 in.		1.0491×2.8128	2.9509 in.
X_F	$r_f(1+M_f\alpha_F \cos \beta_f)$	24a		11.806 (1+3.5×0.4235 cos 16.602)	28.576 in.		19.098 (1+3.5×0.2618 cos 16.602)	35.868 in.
X_I	$r_f(1-M_f\alpha_F \cos \beta_f)$	24b		1.9735 (1-1.4350×0.4235 cos 44.180)	1.113 in.		2.9509 (1-1.2564×0.2618 cos 52.745)	2.363 in.
Initial expansion part								
$\beta_f-\Psi_f$				44.180-10.000	34.180°			
L_s	$d_0 \cot (\beta_f-\Psi_f)$	24c		1.4728 cot 34.180	2.169			
β_n						II, col. 3, $\Psi_f/2=2.500^\circ$		59.970°
$\beta_n-\frac{\Psi_f}{2}$							59.970-2.500	57.470°
w_f	$\frac{A_f}{A_i} A_i=\frac{r_f}{r_i} A_i$						1.0491×1.4728	1.5451
L_s	$d \cot \left(\beta-\frac{\Psi_f}{2}\right)+w_f \cot \beta_f$						1.4728 cot 57.470 1.5451 cot 52.745	2.114
L	$X_F-X_I+L_s$			28.576-1.113+2.169	29.632		35.868-2.363+2.114	35.619

¹ No straight-walled part; initial expansion accomplished by 1 turn about sharp corner.² Straight-walled part with α_F of 15.000°; initial expansion accomplished by 2 turns in succession about sharp corner at each wall.